Title
Stochastic Evolutionary Demography under a Fluctuating Optimum Phenotype

Authors
Chevin, Luis-Miguel
Cotto, Olivier
Ashander, Jaime

Publication Date
2017-09-27

Data Availability
The data associated with this publication are available at: http://dx.doi.org/10.5061/dryad.101h0

Peer reviewed

Stochastic evolutionary demography under a fluctuating optimum phenotype

Luis-Miguel Chevin[1*], Olivier Cotto[1], and Jaime Ashander[2]

*Corresponding author: luis-miguel.chevin@cefe.cnrs.fr

1: CEFE UMR 5175, CNRS - Université de Montpellier, Université Paul-Valéry Montpellier, EPHE, 1919 route de Mende, 34293 Montpellier, CEDEX 5, France

2: CPB: Center for Population Biology, University of California-Davis, Davis, CA 95616, USA and UCLA Ecology & Evolutionary Biology, 610 Charles E Young Drive East, Terasaki Life Sciences Bldg Receiving Dock, Los Angeles, CA 90095

Abstract

Many natural populations exhibit temporal fluctuations in abundance that are consistent with external forcing by a randomly changing environment. As fitness emerges from an interaction between the phenotype and the environment, such demographic fluctuations probably include a substantial contribution from fluctuating phenotypic selection. We study the stochastic population dynamics of a population exposed to random (plus possibly directional) changes in the optimum phenotype for a quantitative trait that evolves in response to this moving optimum. We derive simple analytical predictions for the distribution of log-population size over time, both transiently and at stationarity under Gompertz density regulation. These predictions are well matched by population- and individual-based simulations. The log-population size is approximately reverse gamma distributed, with a negative skew causing an excess of low relative to high population sizes, thus increasing extinction risk relative to a symmetric (e.g. normal) distribution with the same mean and variance. Our analysis reveals how the mean and variance of log population size change with the variance and autocorrelation of deviations of the evolving mean phenotype from the optimum. We apply our results to the analysis of evolutionary rescue in a stochastic environment, and show that random fluctuations in the optimum can substantially increase extinction risk, by both reducing the expected growth rate and increasing the variance of population size by several orders of magnitude.

Keywords: environmental stochasticity, eco-evolutionary dynamics, fluctuating selection, evolutionary rescue, density dependence, environmental autocorrelation.

Short title: Demography under a stochastic optimum

Introduction

Virtually any population dynamic study reveals temporal variation in population size or density, which often appears largely erratic and seemingly random (reviewed by Lande et al. 2003, chapter 1), except in well-characterized cases of deterministic oscillations such as predator-prey cycles or seasonal dynamics. When random fluctuations in abundance occur in populations large enough that demographic stochasticity can be ignored, they are most likely caused by stochasticity in environmental factors that jointly affect the demographic vital rates of all individuals in the population (environmental forcing). Such environmental stochasticity has received increasing attention in the last decades, in particular because of its importance for extinction risk and conservation (Beissinger and McCullough 2002; Boyce 1992; Lande 1993; Lande et al. 2003; Ruokolainen et al. 2009). Although most of this work is based on the assumption that the environmental driver of population dynamics is not autocorrelated through time (white noise), it has been shown both theoretically (Johst and Wissel 1997; Ripa and Lundberg 1996) and empirically (Laakso et al. 2003; Pike et al. 2004) that temporal autocorrelation in the environment, as commonly reported in time series of environmental variables (e.g. Vasseur and Yodzis 2004), may be a strong driver of population dynamics and extinction risk. Furthermore, the eco-evolutionary mechanisms relating stochasticity of environmental variables to fluctuations in population size are often not addressed explicitly in studies of stochastic population dynamics. Here our aim is to address these two issues, by jointly modeling evolution and demography in a temporally autocorrelated environment.

Most classic work in stochastic population dynamics is based on phenomenological models where the underlying mechanism causing environmental stochasticity in population growth rates is not modeled explicitly (reviewed by Lande et al. 2003; Tuljapurkar 1990). Yet it is broadly accepted in ecology that the influence of the environment on fitness and population growth is largely mediated by phenotypic traits, as attested by several recent population dynamic studies in the wild or in the laboratory (Ellner et al. 2011; Ozgul et al. 2010; Ozgul et al. 2012; Pelletier et al. 2007). Indeed, one major way by which a changing environment may change the fitness of an individual (and the mean fitness of a population) is by altering the trait-fitness relationship. In other words, environmental fluctuations in population growth are likely to include a substantial

contribution from randomly fluctuating phenotypic selection. However, despite an increasing number of studies of the interplay between demography and evolution in stochastic environment (Coulson and Tuljapurkar 2008; Engen et al. 2014; Engen et al. 2013; Engen et al. 2011; Engen and Saether 2014; Sæther et al. 2013), some important aspects of the link between fluctuating selection and environmental stochasticity in population dynamics are still not well incorporated in population dynamic theory. One of these features is selection for an optimum phenotype.

Most evolutionary models of phenotypic evolution in temporally or spatially heterogeneous environments assume that one or several quantitative traits are under selection for an optimum phenotype that changes with the environment. This is consistent with a number of well-established empirical facts, from phenotypic stasis in the long run despite the possibility for rapid evolution (Estes and Arnold 2007; Uyeda et al. 2011), to variation in the fitness effects of mutations across environments (Martin and Lenormand 2006a; Martin and Lenormand 2006b), or even direct measurement of fitness and traits across time and environments (Chevin et al. 2015). When the function relating traits to fitness includes an optimum phenotype that changes with the environment, environmental stochasticity causes the optimum to change randomly in time, resulting in randomly fluctuating selection. Evolutionary theory has investigated the expected load caused by maladaptation under different patterns of fluctuations of the optimum phenotype for a quantitative trait. Beyond genetic variance and the strength of stabilizing selection towards the optimum phenotype, the temporal variance and autocorrelation in the optimum appear to be major determinants of the expected load (Charlesworth 1993; Chevin 2013; Lande 1976; Lande and Shannon 1996). Nevertheless, we still lack predictions for how these important elements of evolutionary demography affect population dynamics under environmental stochasticity. In particular, we need to know how much stochastic variance in population size (among replicate evolutionary paths) is generated by random environment-driven fluctuations of an optimum phenotype, because this bears on both the predictability of the population dynamic process, and on the probability of extinction. More generally, the overall shape of the abundance distribution is likely to also be a driver of extinction risk, in particular if it is asymmetric towards low population size.

One situation where the demographic consequences of random fluctuations in an optimum phenotype are likely to play an important role is evolutionary rescue in the face of strong environmental stress. When an abrupt environmental shift induces strong maladaptation that

triggers a population decline, population persistence is only possible if adaptive evolution is rapid enough to restore positive Malthusian fitness before the population has gone extinct. This scenario, described as evolutionary rescue (Gomulkiewicz and Holt 1995), has attracted considerable attention from both theoreticians (Chevin and Lande 2010; Gomulkiewicz and Holt 1995; Gomulkiewicz et al. 2010; Martin et al. 2013; Orr and Unckless 2008; Uecker and Hermisson 2016) and empiricists (Bell and Gonzalez 2009; Ramsayer et al. 2013). Since environmental stochasticity is ubiquitous, its potential importance during evolutionary rescue has been emphasized (Chevin et al. 2013), and recently addressed in the context of evolving plasticity (Ashander et al. 2016), but a more complete characterization of how environmental fluctuations affect the outcome of evolutionary rescue following a major shift in the average environment is still lacking.

Here we develop and analyze an eco-evolutionary model where environmental stochasticity in population dynamics arises from random fluctuations in the optimum phenotype for a quantitative trait, which evolves under density- and frequency-independent selection. We analytically derive the distribution of population size caused by deviations from the fluctuating optimum, first during a transient phase of density-independent population growth – which we use to investigate evolutionary rescue –, and then at stationarity around the carrying capacity under density-dependent growth (but assuming density-independent selection). We compare our analytical predictions to population- and individual-based simulations. We show that in this model, which is consistent with a large body of empirical and theoretical work in evolutionary ecology, the distribution of population size can differ substantially from that in phenomenological models of stochastic population dynamics, with important consequences for extinction risk, in particular during evolutionary rescue, but also at stationarity.

Model

Evolutionary demography

We model evolutionary demography in discrete non-overlapping generations for simplicity, but our model should be a good approximation for overlapping generations without age structure, that is, when vital rates (survival and fecundity) do not vary systematically with age. Age-structured evolutionary demography in stochastic environments has additional complications

introduced by fluctuations in the age structure itself (Engen et al. 2011; Engen et al. 2009; Sæther et al. 2013), and thus requires further developments. We will also assume that the population is large enough to neglect demographic stochasticity (randomness in the reproductive success of individuals with the same phenotype in the same environment), such that all variation in population size comes from environmental factors jointly affecting all individuals in the population. However, we also use individual-based simulations to examine the robustness of our analysis to this assumption.

Following earlier work in evolutionary genetics (e.g. Arnold et al. 2001; Chevin 2013; Lande 1976; Wright 1935) and evolutionary demography (Gomulkiewicz and Holt 1995; Gomulkiewicz and Houle 2009; Lande and Shannon 1996; Lynch and Lande 1993), we assume that fitness depends on the match between an individual's phenotype and an optimum phenotype set by the environment. We model the fitness peak around this optimum phenotype using a Gaussian fitness function, which is the most commonly used function because (i) it has useful mathematical properties, (ii) it can approximate many continuous functions with a peak near the optimum (by Taylor series on the log scale), and (iii) has proved to provide a better fit to data on fitness effects of mutations across environments than other shapes with more abrupt reductions of fitness away from the peak (Martin and Lenormand 2006a). Following Chevin & Lande (2010), we thus assume the absolute multiplicative fitness (expected number of offspring) of an individual with trait value z in a population of size (or density) N is

$$R(z,N) = \exp\left\{-\frac{(z-\theta_t)^2}{2\omega^2}\right\} R_m^{1-g(N)/g(K_m)}. \quad (1)$$

The first factor on the right-hand side, which we will denote as $W(z)$, corresponds to stabilizing selection on phenotype z through a Gaussian peak of width ω and optimum phenotype θ_t that changes in time because of changing environment (hence the subscript t, which is omitted from other variables for simplicity). Note that we assume for simplicity that the shape of the fitness function is unchanged by the environment. The second factor on the right-hand side accounts for competition-mediated density-dependence of population growth. The form of density dependence is specified by $g(N)$, an increasing positive function of N. The parameter K_m (where m is for maximum) is the equilibrium population size (carrying capacity) of a hypothetical population where all individuals have the optimum phenotype at all times. We assume that K_m is

large enough that $\lim_{N\to 0} g(N) << g(K_m)$. Hence the multiplicative growth rate at low densities (or intrinsic rate of multiplicative increase) for a population where all individuals have the optimal phenotype is R_m.

The mean absolute multiplicative fitness in a population polymorphic for phenotype *z* is $\overline{R} = R_m^{1-g(N)/g(K_m)}\overline{W}$, where $\overline{W} = \int_{-\infty}^{\infty} p(z)W(z)dz$, and *p*(*z*) is the phenotype distribution (probability density function). The relative fitness is thus $w(z) = R/\overline{R} = W/\overline{W}$, which depends on individual phenotype but not population density. Hence, as noted earlier about this model and related ones in continuous time (Case and Taper 2000; Kirkpatrick and Barton 1997; Ronce and Kirkpatrick 2001), selection is here density- and frequency-independent, even though population growth is density regulated. This allows the evolutionary dynamics to be tracked first without reference to population size, and then combined with the demographic model to produce the population dynamics. The fitness function in (1) applies best when the two terms on the right hand side correspond to two different events in the life cycle, for instance phenotype-independent density regulation followed by density-independent viability selection, with census size measured prior to both events. In the more general case where selection is also density dependent, demographic fluctuations caused by stochastic fluctuations in the optimum feed back on evolution, and the variance of these fluctuations determines the ESS life history, over a continuum from *r*- to *K*-strategies (Engen et al. 2013; Lande et al. 2009).

The evolutionary dynamics can be analyzed most straightforwardly by assuming a normally distributed trait, with mean $\bar{z}$ and phenotypic variance *P*, as is common practice for polygenic quantitative traits (Falconer and MacKay 1996; Lynch and Walsh 1998). The mean 'evolutionary' fitness then is $\overline{W} = \sqrt{S\omega^2}\exp(-S(\bar{z}-\theta)^2/2)$, with $S = (\omega^2 + P)^{-1}$ the strength of stabilizing selection, which is assumed small. The response to selection by the mean phenotype over one generation is $\Delta\bar{z} = -GS(\bar{z}-\theta)$, with *G* the additive genetic variance of the trait (Lande 1976). Such a model has previously yielded analytical results for the expected long-term fitness and evolution of a population in a stochastic environment (Bürger and Lynch 1995; Chevin 2013; Lande and Shannon 1996; Lynch and Lande 1993), assuming a constant additive genetic variance. We will use the same assumptions here to derive more general analytical results about

the complete distribution of fitness and population size. The robustness of our assumptions will then be investigated using individual-based simulations.

It is convenient to express the demographic recursions on the logarithmic scale (Chevin and Lande 2010; Lande et al. 2003). Writing $n = \ln N$, the basic recursion $N_{t+1} = \overline{R} N_t$ leads to

$$n_{t+1} - n_t = r_m[1 - g(N_t)/g(K_m)] - \frac{1}{2}\ln(1 + P/\omega^2) - \frac{S}{2}(\bar{z} - \theta)^2, \quad (2)$$

with $r_m = \ln R_m$. Most of our analytical results rely on an approximation of weak density dependence ($g(N_t)/g(K_m) << 1$), which is valid for $N << K_m$ at all times. In practice, this will be a good approximation when a population colonizes a previously empty patch, or when substantial maladaptation causes the population to remain well under the carrying capacity for large amounts of time, as in the scenario of evolutionary rescue we analyze below. How well this approximation performs also depends on the form of density dependence, as we will also investigate.

Neglecting density dependence, the population dynamics on the log scale becomes

$$n_t = n_0 + (r_m - L_V)t - \frac{S}{2}Q_{t-1}, \quad (3)$$

where $Q_t = \sum_{k=0}^{t} x_k^2$, and $x_k = \overline{z_k} - \theta_k$ is the deviation of the mean phenotype from the optimum at time *k*. The term $L_V = \ln(1 + P/\omega^2)/2 \approx P/(2\omega^2)$ in eq. (3) (where the approximation is under weak stabilizing selection) is the variance load, which accounts for the fact that mean fitness is always below its maximum in a population with phenotypic variance, because some phenotypes deviate from the optimum even when the mean phenotype does not (e.g., Bürger and Lynch 1995; Lynch and Lande 1993). The third term on the right hand side is the cumulative lag load, caused by maladaptation of the mean phenotype (deviations from the optimum) across generations. This cumulative lag load will be our main focus here, as it results from the interplay between environmentally induced changes in the optimum and tracking of this optimum by the mean phenotype through genetic evolution.

Environmental fluctuations

We focus on a stochastic environment that is temporally autocorrelated. More specifically, we assume that the optimum follows an autoregressive process of order 1 (AR1), such that the environment at a given time step tends to resemble that in the previous time step, with a degree of resemblance - and hence of environmental predictability - controlled by a parameter that tunes the amount of autocorrelation. Such a model, which was previously investigated in related evolutionary models (Charlesworth 1993; Chevin 2013; Lande and Shannon 1996; Tufto 2015), causes a geometric decrease with time of autocorrelation in the optimum phenotype. Although more complex forms of autocorrelation could also have been considered, and have been documented for environmental variables (Halley 1996; Vasseur and Yodzis 2004), they may not be empirically detectable for fluctuations of an optimum phenotype, while an AR1 in the optimum has already been detected and parameterized (Chevin et al. 2015).

In this context, it has been shown previously (e.g., Chevin 2013; Lande and Shannon 1996; Lynch and Lande 1993) that both the mean phenotype $\bar{z}$ and the deviation from the optimum $x = (\bar{z} - \theta)$ follow stationary Gaussian processes. We introduce the vector $\mathbf{x}_t$, whose elements are deviations from optimum x_k (ordered chronologically) from time 0 to time *t* (inclusive). Vector $\mathbf{x}_t$ is thus a multivariate Gaussian random variable of length $t+1$, with mean $\boldsymbol{\mu}_t$ and variance-covariance matrix $\mathbf{X}_t$. Hence for any $t \geq 0$, $Q_t = \mathbf{x}_t^T \mathbf{x}_t$ (with ^{T} denoting vector or matrix transposition) is a quadratic form in Gaussian vectors, a scalar random variable whose distribution is well characterized, notably through all its moments (Mathai and Provost 1992). In particular, we have for the mean and variance (Mathai and Provost 1992)

$$\mathrm{E}(Q_t) = \boldsymbol{\mu}_t^T \boldsymbol{\mu}_t + tr(\mathbf{X}_t) \tag{4a}$$

$$\mathrm{V}(Q_t) = 4\boldsymbol{\mu}_t^T \mathbf{X}_t \boldsymbol{\mu}_t + 2tr(\mathbf{X}_t^2), \tag{4b}$$

where *tr*() is the trace of a matrix, the sum of its diagonal elements (or of its eigenvalues).

Because we assume stationarity for the stochastic component of variation in the optimum and for deviations of the mean phenotype from this optimum, the stochastic variance of x_t is the same for all *t*, such that all diagonal elements of $\mathbf{X}_t$ are equal to σ_x^2. We can thus work with the scaled vector $\mathbf{y}_t = \sigma_x^{-1} \mathbf{x}_t$, whose covariance matrix $\mathbf{Y}_t = \sigma_x^{-2} \mathbf{X}_t$ is the autocorrelation matrix of

$\mathbf{x}_t$. Hence, all diagonal elements of $\mathbf{Y}_t$ are 1, while any off-diagonal element $Y_t(i, j)$ with $i \neq j$ is the temporal autocorrelation of deviations from the optimum over time lag |*i*-*j*|. This entails that $tr(\mathbf{Y}_t) = t+1$, and hence

$$tr(\mathbf{X}_t) = \sigma_x^2(t+1). \tag{5a}$$

We also have $\mathbf{X}_t^2 = \sigma_x^4 \mathbf{Y}_t^2$, and denoting as λ_i the i^{th} eigenvalue of $\mathbf{Y}_t$, it is easily shown by diagonalization that $tr(\mathbf{Y}_t^2) = \sum \lambda_i^2 = (t+1)\mathrm{E}(\lambda^2)$. Furthermore $\mathrm{E}(\lambda) = 1$ (since all diagonal elements are 1), so for large enough *t* (such that $t+1 \approx t$), we may also write $\mathrm{E}(\lambda^2) = 1 + \mathrm{V}_{\lambda,t}$, where $\mathrm{V}_{\lambda,t}$ is the variance of λ_i, leading to

$$tr(\mathbf{X}_t^2) = \sigma_x^4(t+1)(1+\mathrm{V}_{\lambda,t}). \tag{5b}$$

Furthermore, since the trace of a matrix product is the sum of its term-by-term products, we also have

$$tr(\mathbf{X}_t^2) = \sigma_x^4\left(t+1+2\sum_{i=0}^{t}\sum_{j=i+1,}^{t} Y_{ij}^2\right) = \sigma_x^4(t+1)[1+2\mathrm{E}_{i\neq j}(Y_{ij}^2)t]. \tag{5c}$$

Comparison of eqs (5b) and (5c) shows that the variance in eigenvalues of $\mathbf{Y}_t$ equals twice the mean squared off-diagonal element of $\mathbf{Y}_t$, multiplied by *t*. This shows that the larger the autocorrelation in maladaptation (in absolute value), the larger squared off-diagonal elements in $\mathbf{Y}_t$, and hence the larger $\mathrm{V}_{\lambda,t}$ and $tr(\mathbf{X}_t^2)$ for a given time *t*.

We also consider the situation where a deterministic forcing causes the mean optimum to change over time, but the stochastic component of environmental variation in the optimum remains unchanged, that is, deviations of the optimum phenotype from its current mean retain their stationary distribution (as in Chevin 2013; Lynch and Lande 1993). This allows us to investigate how environmental stochasticity affects the outcome of evolutionary rescue following a major environmental change causing an abrupt shift in the average optimum.

Results

Our main goal is to find the distribution of population size over time, conditional on knowledge of the initial population size N_0. This is relevant to any empirical situation (either experimental or

in the wild) where the population size/density is censused or estimated at time 0, and the aim is to predict the future fate of the population. This means that the initial distribution of population size is a spike at N_0 (technically speaking, a Dirac delta), and then expands over time because of environmental stochasticity causing uncertainty in future population sizes. We compare our analytical results to population- and individual-based simulations (see Appendix for details of the simulation method). The former allows testing precise predictions of the model with a high level of replication, under the assumption that all stochasticity originates from the environment (i.e., no genetic drift or demographic stochasticity). The latter allows investigating other sources of stochasticity not accounted for in our analytical treatment (genetic drift and demographic stochasticity).

Density independent population dynamics

Distribution of population size at time t

Under density independent growth (eq. 3), the expected population size under a fluctuating optimum is, from eqs (3-5),

$$\mathrm{E}(n_t) = n_0 + (r_m - L_V)t - \frac{S}{2}\left(\sum_{k=0}^{t-1} \mathrm{E}[(\bar{z} - \theta)_k]^2 + \sigma_x^2 t \right) \qquad (6a)$$

Eq. (6a) shows that the expected population size (on the log scale) is reduced (beyond the effect of the variance load L_V) by (i) any deterministic forcing (such as a trend or a sudden shift) causing non-zero phenotypic maladaptation on average (first term, obtained by expanding the quadratic form for the mean of the process); (ii) stochastic fluctuations in the optimum causing variance in phenotypic maladaptation (second term). This second effect, which arises because of the negative curvature of the fitness landscape close to an optimum phenotype (just like the variance load), reiterates findings from previous studies of evolutionary demography (Bürger and Lynch 1995; Lande and Shannon 1996; Lynch and Lande 1993).

An important quantity that was not derived in previous theory is the variance in population sizes among replicates, which quantifies the extent to which environmental stochasticity in the optimum translates into randomness in population dynamic trajectories. For a given expected population size, larger variance makes it more likely that some stochastic paths will lead to populations with very low size, and thus high extinction risk. From eqs. (3-5) the variance in log-population size at time *t* is

$$\mathrm{V}(n_t) = S^2\left(\sigma_x^2 \boldsymbol{\mu}_{t-1}^T \mathbf{Y}_{t-1} \boldsymbol{\mu}_{t-1} + \frac{1+\mathrm{V}_{\lambda,t-1}}{2}\sigma_x^4 t\right), \quad (6b)$$

where $\boldsymbol{\mu}_{t-1}$ is the vector of expected (deterministic) deviations from the optimum up to time $t-1$, $\mathbf{Y}_{t-1}$ is the matrix of autocorrelation of deviations from optimum between different generations, and $\mathrm{V}_{\lambda,t-1}$ is the variance of eigenvalues of this matrix (when t is not much larger than 1, the term $1+\mathrm{V}_{\lambda,t-1}$ should be replaced by the more accurate $\mathrm{E}(\lambda^2)$ in equation 6b and others below). Equation (6b) offers several useful insights. First, the *expected* phenotypic maladaptation $\boldsymbol{\mu}_{t-1}$ has an effect on the *variance* of population size (first term on right-hand side). This implies that a deterministic trend in the optimum may cause the variability in population dynamic trajectories to increase. Second, all else being equal, the randomness in population dynamics is larger when maladaptation is more autocorrelated in time (second term on right-hand side). This occurs because the variance $\mathrm{V}_{\lambda,t-1}$ of eigenvalues in eq. (6b) is larger when temporal autocorrelation of maladaptation (off-diagonal elements of $\mathbf{Y}_{t-1}$) have larger absolute values (below eq. 5c).

All other moments of the distribution of the log-population size n can be retrieved by applying the theory of quadratic forms in random vectors (Mathai and Provost 1992) to eq. (3). However, rather than providing here the general formula for moments of n, we instead use an approximation for the whole distribution. This approximation relies on the fact that, in the absence of temporal autocorrelation in phenotypic maladaptation, the quadratic form Q_{t-1} in eq. (3) is a sum of t squared independent Gaussian variables with same variance σ_x^2 but different means. We can thus write $Q_{t-1} = \sigma_x^2 \chi^2_{t-1,q}$, where $\chi^2_{t,q}$ is a non-central chi-square variable with t degrees of freedom and non-centrality parameter $q = \boldsymbol{\mu}_{t-1}^T \boldsymbol{\mu}_{t-1} / \sigma_x^2$. With autocorrelation in maladaptation, $\mathbf{Y}$ is no longer diagonal but still positive semi-definite, so Q_{t-1} is the sum of squared *non-independent* Gaussian variables (again with same variance σ_x^2). However, there is always a transformed space where Q_{t-1} can be written as a sum of independent squared Gaussian variables but with different variances, i.e., a weighted sum of non-central chi-square variables with 1 degree of freedom (Mathai & Provost 1992). Because a chi-square distribution is a special

case of gamma distribution, a natural choice to approximate the distribution of Q_{t-1} (and thus of n_t) in the general case is a gamma distribution (as used by Martin and Lenormand 2006b in a different context that also involved Gaussian stabilizing selection). This distribution has just two parameters, a shape parameter κ and scale parameter ν, and has mean $\mathrm{E}[Q] = \kappa\nu$ and variance $\mathrm{V}[Q] = \kappa\nu^2$. We can thus define the parameters of the gamma distribution from the first two moments, namely $\kappa = \mathrm{E}[Q]^2 / \mathrm{V}[Q]$ and $\nu = \mathrm{V}[Q] / \mathrm{E}[Q]$.

Using eqs (4-5), we can then write the probability density function of log population size at time *t* under density-independent population growth as

$$f_t(n_t) = \gamma_{\kappa_t,\nu_t}(n_0 + (r_m - L_V)t - n_t) \tag{7}$$

where $\gamma_{\kappa,\nu}$ is the probability density of a gamma variable with shape parameter κ and scale parameter ν. Note that the minus sign before n_t in the expression for $f_t(n_t)$ indicates that the gamma distribution for n_t is reversed. The parameters of this gamma distribution follow from the dependence of n_t on Q_{t-1} (eq. 3), yielding

$$\kappa_t = \frac{\mathrm{E}(Q_{t-1})^2}{\mathrm{V}(Q_{t-1})} \tag{8a}$$

$$\nu_t = \frac{S}{2}\frac{\mathrm{V}(Q_{t-1})}{\mathrm{E}(Q_{t-1})}$$

where the moments of Q are provided in eqs. (4-5). In particular, under purely stochastic variation in the environment (no deterministic change in the optimum, $\boldsymbol{\mu}_t = 0$ for all *t*), the shape and scale parameters of the gamma distribution in eq. (7) are simply

$$\kappa_t^* = \frac{t}{2(1 + \mathrm{V}_{\lambda,t-1})} \tag{8b}$$

$$\nu_t^* = S\sigma_x^2(1 + \mathrm{V}_{\lambda,t-1}).$$

Equations (7-8) are among our main result. They indicate that, when stochasticity in population dynamics is caused by random fluctuations of an optimum phenotype in the form of a Gaussian process, the distribution of log population size under density-independent growth can be approximated by a displaced and reversed gamma distribution, which is fully characterized by its scale and shape parameters. This has several implications, which contrast with the commonly

assumed log-normal distribution for multiplicative growth rates, leading to normally distributed log-population size under density independent growth (Lande et al. 2003 and references therein). First, the distribution in eq. (7) is right-bounded, since no population can grow faster than one where the mean phenotype is always at the optimum, for which $n_t = n_0 + (r_{\max} - L_V)t$. Second, the distribution of n_t is skewed to the left (since it is a reversed gamma), that is, it is asymmetric towards lower population sizes. This is particularly important considering that low population sizes are what matters most for conservation purposes. In more quantitative terms, the skewness parameter (third moment scaled by the standard deviation to the power 3) of a gamma distribution is $2/\sqrt{\kappa}$. Under purely stochastic variation in the optimum ($\boldsymbol{\mu} = 0$), the skewness of the distribution is thus $-\sqrt{8[1+\mathrm{V}_{\lambda,t-1}]/t}$ (the minus sign is because the gamma is reversed in eq. 7). Therefore, the distribution of population size is more skewed when maladaptation is more strongly autocorrelated between generations (larger $\mathrm{V}_{\lambda,t-1}$). This asymmetry in the distribution of n_t decrease with time, but slowly (as $t^{-1/2}$), implying that population sizes well below the expectation are likely to occur over a substantial time, even when starting from a large population. Eventually, as time (and thus the shape parameter of the gamma) tends to infinity, the distribution of n_t tends to a Gaussian (gamma with large shape parameter), as a consequence of the central limit theorem.

Figure 1 shows how the prediction in eqs (6-8) matches the distribution of the log population size under density-independent growth, in population-based simulations under a stochastic optimum. As a comparison, we have also plotted the distribution in a phenomenological model where the multiplicative growth rate is assumed to be log-normally distributed with same mean and variance, leading to a Gaussian distribution of log-population size. The distribution of log population size under a fluctuating optimum phenotype (conditional on the initial condition n_0) is very skewed, and differs markedly from a Gaussian in the early generations (upper panels). Furthermore, in this example where autocorrelation in the optimum is not negligible ($\rho = 0.5$), the skewness in the population size distribution is maintained even after 50 generations of eco-evolutionary dynamics (a large time in typical population dynamic studies). In particular, the tail on the left remains fatter than for Gaussian, and this increased

probability of low population size is well captured by our gamma approximation (inset in lower panel of Figure 1).

Stochastic dynamics of maladaptation

The distribution of population size in eqs (6-7) crucially depends on the temporal variance and autocorrelation of deviations of the mean phenotype from the optimum. In the absence of additive genetic variance for the trait, these parameters are entirely determined by patterns of environmental fluctuations in the optimum, and our model then directly compares to stochastic population dynamic models without evolution (as reviewed in Lande et al. 2003). In contrast, with additive genetic variance in the trait, maladaptation at any time depends on the interplay between environmentally driven changes in the optimum and evolutionary responses to fluctuating selection. We can then use results from previous theory of evolution of quantitative traits in stochastic environments to retrieve quantities of interest. In particular, Chevin and Haller (2014) derived the variance and autocorrelation function of directional selection gradients on a quantitative trait under random fluctuations of an optimum phenotype, following different types of Gaussian processes (formulas in their Table 1). Since the directional selection gradient is the mean deviation from the optimum multiplied by a factor S (the strength of stabilizing selection), the variance in maladaptation σ_x^2 is simply obtained by dividing the variance of selection gradients by S^2, while the autocorrelation in maladaptation that enters matrix $\mathbf{Y}$ is the same as the autocorrelation of selection gradients. In particular, for an autoregressive optimum (AR1), the variance of deviations from the optimum is

$$\sigma_x^2 = \frac{\sigma_\theta^2}{1+SGT}, \tag{9a}$$

where σ_θ^2 is the stationary variance of the optimum phenotype, and $T = -1/\ln\rho$ is a characteristic time scale of autocorrelation in the optimum (ρ is the autocorrelation of the optimum over one time step). The autocorrelation of deviations from optimum between generations i and j is

$$Y_t(i,j) = \frac{e^{-|i-j|/T} - SGTe^{-SG|i-j|}}{1-SGT}. \tag{9b}$$

As noted by Chevin & Haller (2014), this autocorrelation function can be approximated at small times ($|i-j|$ smaller than T and $1/SG$) by

$$Y_t(i,j) \approx e^{-(SG+1/T)|i-j|} \approx U^{|i-j|}, \quad (9c)$$

where $U = (1-SG)\rho$. Values of σ_x^2 and $\mathbf{Y}$ under other forms of fluctuations in the optimum (white noise, random walk) can be retrieved similarly from Table 2 in Chevin and Haller (2014).

Equations (9a,b) show that the environmental variance and autocorrelation in the optimum do not directly translate into variance and autocorrelation in maladaptation (which ultimately affect population size, eq. 6-7). For instance, stronger positive autocorrelation in the optimum allows for better adaptive tracking through genetic evolution (smaller σ_x^2 for larger T), which reduces the *variance* of deviations from the optimum. This effect may well dominate the effect of increased *autocorrelation* of *x* at larger T, and thus lead to decreased rather than increased variance of n_t under stronger autocorrelation in the optimum (eq. 6a).

Positive autocorrelation in the optimum thus has antagonistic effects on the population dynamics. On the one hand, by allowing for better adaptive tracking (in the presence of genetic variance), it reduces the variance in mismatch with the optimum, thus decreasing both the mean and variance of the cumulative lag load (eq. 6a,b), and hence extinction risk. On the other hand, autocorrelation in the optimum generates autocorrelation in deviations from the optimum (more so when genetic variance is lower, Chevin and Haller 2014), which increases the variance among stochastic population dynamic paths (eq. 6b), thus increasing extinction risk.

Evolutionary rescue with environmental stochasticity

We now apply our framework to analyze evolutionary rescue mediated by evolution of a polygenic quantitative trait in the face of a major abrupt environmental shift combined with stochastic environmental fluctuations in the optimum. This major environmental shift, beyond the usual range of random fluctuations, is modeled as a displacement of the mean optimum by an amount δ at time 0. Following classical quantitative genetic results based on recursions, assuming constant genetic variance, of the simple evolutionary equation above for $\Delta\bar{z}$ (Gomulkiewicz and Holt 1995; Lande 1976), the expected deviation from the optimum decays geometrically over time, $\mathrm{E}(x_t) = \delta(1-GS)^t$. As the $\mathrm{E}(x_t)$ are the components of the vector $\boldsymbol{\mu}$, we have

$$\boldsymbol{\mu}_{t-1}^T \boldsymbol{\mu}_{t-1} = \delta^2 \sum_{k=0}^{t-1} (1-GS)^{2k} = \frac{\delta}{GS(2-GS)}[1-(1-GS)^{2t}], \quad (10)$$

which may be approximated as $\delta[1-\exp(2GSt)]/(2GS)$ under weak stabilizing selection (small GS). Figure 2A shows the evolutionary dynamics for the expected mean phenotype (red line, from eq. 10), and for individual stochastic trajectories of the mean phenotype (black lines), under an optimum with a mean that is shifted by $\delta = 4$ at generation 0, and fluctuates around this new mean with a given variance an autocorrelation. Combining the expected trajectory in eq. (10) with the dynamics of the distribution of population size in eqs (6-7) provides us with the distribution of population size during the process of ER in a stochastic environment.

Figure 2B shows the population dynamics for 500 simulated populations (gray lines), together with quantile envelopes (black lines) based on the predicted distribution of log population size in eqs. 6-7. This illustrates two detrimental consequences of environmental stochasticity for evolutionary rescue. First, random fluctuations in the optimum reduce the expected growth rate of the population (eq. 6a), causing the expected population size to be smaller than in a model without a fluctuating optimum (compare blue and red lines). And second, environmental stochasticity causes variance in population sizes at any time, because of chance in the series of environments encountered by each eco-evolutionary path. Importantly, because of the exponential nature of population growth, this effect of environmental stochasticity can cause population sizes to span several orders of magnitude at any given time (as in our example), and in particular at the critical time for evolutionary rescue when population size reaches its minimum (towards generation 30 in Figure 2). The variance in population dynamics caused by the fluctuating optimum may thus contribute substantially to the probability of extinction and ER.

Our analysis can provide metrics for extinction risk during the process of ER. We cannot derive an actual probability of extinction because we neglect demographic stochasticity caused by finite population size, and because our quantitative genetic assumptions are not valid at very low population size. At any rate, it can be argued that below a critical population size (say, a few tens or hundreds of individuals), evolutionary processes such as adaptation to a changing environment are not the most crucial determinants of population persistence, and purely demographic phenomena such as Allee effects, demographic stochasticity or habitat fragmentation become the dominant factors of extinction risk (Lande 1988). Following earlier studies (Ashander et al. 2016 ; Chevin and Lande 2010; Gomulkiewicz and Holt 1995), we thus focus instead on the probability that the population decays below a critical size N_c, below which

extinction risk is assumed to be high because of these purely demographic factors. Using the analytical distribution in eq. (7), the critical probability that the population size is below N_c is

$$P_{crit} = \frac{\Gamma(\kappa, [n_0 + (r_m - L_V)t - \ln N_c]\nu^{-1})}{\Gamma(\kappa)}, \quad (11)$$

where $\Gamma()$ and $\Gamma(,)$ are Euler's gamma function and incomplete gamma function, respectively. We suggest that max(P_{crit}), the maximum critical probability over time, is a good predictor of extinction risk; conversely $1 - \max(P_{crit})$ should be a good predictor of the probability of evolutionary rescue.

Figure 3 shows how P_{crit} changes over time in scenarios of evolutionary rescue with a stochastic optimum, comparing the analytical prediction in eq. (11) to population-based simulations. Figure 3A shows that the variance in the optimum has a dramatic impact on the probability of ER. In the context modeled in this figure, P_{crit} would remain vanishingly small in the absence of fluctuations in the optimum, such that a purely deterministic model would predict certain ER (no extinction risk), but changing the variance in the optimum strongly impacts the maximum extinction risk P_{crit} (and to a lesser extent, the time at which this maximum P_{crit} is encountered). For instance, the maximum P_{crit} is almost doubled as the variance in optimum changes from 1 to 4 (compare green and red lines). Note that the range of fluctuations we considered is moderate: the expected load (in Malthusian fitness per generation) caused by the random optimum, $S\sigma_x^2/2$, only varied from 0.0047 to 0.0748.

Figure 3B shows that the autocorrelation in the optimum has a more moderate impact on extinction risk during ER. Higher autocorrelation results in slightly higher maximum P_{crit}, but mostly increases the duration over which P_{crit} remains large. This can increase extinction risk, by exposing the populations to hazardous sizes for longer. Both effects of environmental autocorrelation on P_{crit} during ER result mostly from the higher variance in population size under higher autocorrelation in the optimum (and in deviations from the optimum, see eq. 9b).

Including density dependence

So far our analysis has assumed density-independent population growth. Density-dependent regulation resulting from intraspecific antagonistic interactions (e.g. resource competition) further reduces vital rates and population size, beyond the effect of maladaptation. The extent to which this effect is mostly restricted to large population sizes near the carrying capacity depends

on the shape of the density dependence function $g(N)$ in eqs. (1-2). At one extreme, models of ceiling density dependence (as used by e.g. Lande 1993) assume that competition only exists at carrying capacity, while population growth is unregulated for any population size below carrying capacity (that is, competition strength is a step function of population size/density). At the opposite end of the spectrum, competition strength decays only logarithmically with decreasing population size (Gompertz model). In between these extremes, a range of situations can be explored using the so called theta-logistic model of Gilpin and Ayala (1973), for which $g(N) \propto N^{\Theta}$ in eq. (2). This model includes the logistic model when $\Theta = 1$, tends to the ceiling model when $\Theta >> 1$, and to the Gompertz model when $\Theta \to 0$ (for further discussion, see Lande et al 2003, or Chevin and Lande 2010 in the context of evolutionary rescue). Note that here, as in Chevin and Lande (2010), we use a discrete-time version of the theta-logistic model, which for $\Theta = 1$ is the Ricker model (discrete-time analog to the logistic model).

Transient dynamics: stochastic evolutionary rescue with density dependence

During a transient process such as evolutionary rescue, density dependence reduces the population size below what is predicted in a density-independent model (e.g., Chevin and Lande 2010). Including density dependence substantially complicates the analysis of the transient population dynamics analyzed above. However, we can use a heuristic argument to understand the impact of density dependence on extinction risk. This argument relies on the fact that the lower tail of the distribution of population size consists of stochastic paths that experienced a series of bad environments, causing them to decline more rapidly than average. They should thus have experienced weaker-than-average density-dependent competition in their demographic history. Therefore in populations that undergo density-dependent growth, predictions that assume density-independence (as we derived above) should apply better to the lower tail than to the rest of the distribution of log population size. This is especially true when the expected population size is below carrying capacity because of stress, as occurs during ER. However, the extent to which this argument holds should depend on the form of density dependence, which determines whether the demographic impact of competition is limited to population sizes near the carrying capacity.

Figure 4 shows how extinction risk during ER, as quantified by the maximum P_{crit} over time, depends on the form of density dependence. Note that with population dynamics defined by

equation (2), the equilibrium population size in a constant environment does not equal K_m, since it is reduced by the variance load. In a stochastic environment, the expected population size is further reduced by the expected stochastic load $S\sigma_x^2/2$. To ensure that the equilibrium population size was the same when varying the form of the density dependence, we set the equilibrium (and initial) population size to $K = 10000$, and then rescaled the carrying capacity of a well-adapted population to $K_m = K[(r_m - L_V - S\sigma_x^2/2)/r_m]^{1/\Theta}$, following Chevin and Lande (2010). Consistent with our heuristic argument, extinction risk quantified by the maximum P_{crit}, increases as the exponent Θ of the density regulation function decreases (Figure 4). Indeed as the exponent Θ increases, density dependence becomes more and more narrowly restricted to population sizes near the carrying capacity, and P_{crit} thus decreases towards its density-independent value predicted by our analytical results. In the limit of ceiling regulation, extinction risk is very well predicted by our analytical P_{crit}. In this case, the distribution of population size is similar to $f(n_t)$ in eq. (7), but truncated at ln(K). Hence this form of density dependence will not affect the extinction probability, which concerns the other extremum of the distribution.

Long-term stationary distribution

In the long run, if the expected growth rate of a population is positive, population size will reach a stationary distribution close to the carrying capacity, with breadth determined by the magnitude of environmental fluctuations in population growth rate relative to the strength of density dependence. Lande et al. (2003) have derived this distribution analytically under Gompertz regulation (linear density dependence on the log scale), in a phenomenological model where the distribution of population growth rates is postulated *a priori*, and assuming no autocorrelation in population growth rates. We here extend these results to the situation where stochasticity in population growth rate is generated by evolutionary dynamics under a fluctuating optimum phenotype, with arbitrary autocorrelation of this optimum. In the Appendix, we show that the expected log population size under Gompertz regulation is

$$\mathrm{E}(n) = \ln K, \text{ with } K = K_m^{1-\frac{L_v + S\sigma_x^2/2}{r_m}} \quad . \qquad (12a)$$

Equation (12a) shows that the equilibrium mean population size under Gompertz regulation is reduced by the variance in deviations from the fluctuating optimum, regardless of the autocorrelation of these deviations. The stationary variance is shown in the Appendix to be

$$\mathrm{V}(n) \approx \frac{S^2\sigma_x^4}{2}\frac{1-(\phi-1)U^2}{[1+(\phi-1)U^2](2-\phi)\phi}, \qquad (12b)$$

where $\varphi = r_m / \ln K_m$ quantifies the strength of density dependence , and $U = (1-SG)\rho$, as defined below eq. (9c) (recall that ρ is the autocorrelation of the optimum phenotype over one generation). The stationary distribution of log population is again well approximated by a displaced gamma,

$$f^*(n) = \gamma_{\kappa^*,\nu^*}\left(\frac{r_m - L_v}{\varphi} - n\right) \qquad (13a)$$

where γ_{κ^*,ν^*} is the probability density of a gamma variable with shape and scale parameter κ^* and ν^*, with

$$\kappa^* = \frac{1}{2}\frac{[1+(\phi-1)U^2](2-\phi)\phi}{1-(\phi-1)U^2}, \qquad (13b)$$

and $\nu^* = S\sigma_x^2/(2\varphi\kappa^*)$. Importantly, the shape parameter of the distribution of population size does not increase indefinitely over time here, contrary to the case of density-independent growth. Instead, it reaches a limit that depends on the strength of density dependence, quantified by ϕ. The distribution of log-population size can therefore remain skewed downwards indefinitely.

The predicted distribution in eqs (13a,b) is compared to population-based simulations in figure 5, showing that the approximation performs well under our assumption of weak stabilizing selection. As predicted by eq. (13b), the shape parameter becomes smaller (more skewed distribution) as the strength of density dependence increases. This occurs because the extent to which the current population size is influenced by past maladaptation now depends on the strength of density dependence (weighted sum of x^2 in eq. A2 of the Appendix). In the limit of very weak density dependence ($\varphi \to 0$), all squared deviations from optimum weigh equally, regardless of when they occurred, and we recover a model similar to the density-independent one (eq. 3), where the shape of the gamma distribution increases with time, thus tending towards normality for the asymptotic stationary distribution (but this asymptotic distribution is reached over a very long time, proportional to $1/\varphi$). In the opposite limit of very strong density dependence ($\varphi \to 1$), all memory of past population dynamics is erased in each generation, and only maladaptation in the previous generation matters, resulting in a very skewed stationary

gamma distribution with small shape parameter (similar to a chi-square with 1 degree of freedom). More generally with density-dependent regulation, the asymptotic distribution of population size is always under stronger influence from more recent maladaptation, but more so under stronger density dependence (larger φ), so all things being equal the distribution is more skewed under stronger density dependence. Furthermore, the distributions in Figure 5 are more skewed under higher autocorrelation of the optimum (and deviations from the optimum). The reason is that with stronger autocorrelation, maladaptation is more similar across years, so the effective number of years that are summed is smaller (in the same way as pseudo-replication reduces the effective sample size in statistical analysis), resulting in a gamma distribution with smaller shape parameter.

The autocorrelation of this stationary distribution, which determines the extent to which population size variation is predictable across generations, also can be derived in this model. In the Appendix, we show that the autocorrelation of *n* for populations τ generations apart is

$$\rho_n(\tau) = \frac{\xi(1-\phi)^\tau + \psi U^{2\tau}}{\xi + \psi}, \qquad (14)$$

where $\xi = (U^4 - 1)(\phi - 1)$ and $\psi = U^2(\phi - 2)\phi$. Equation (14) shows that under a fluctuating optimum phenotype and Gompertz density regulation, the time scale of autocorrelation in log population size is smaller when density dependence is stronger (large ϕ), when the autocorrelation in the optimum is weak, and/or the potential for responses to selection is large (that is, $U = (1 - SG)\rho$ is small). The good correspondence between the prediction in eq. (14) and population-based simulations with constant variance is shown in the insets of Fig 5. Note that a large number of generations are needed to accurately estimate the temporal autocorrelation.

Robustness to assumptions and individual-based simulations

Finally, we used individual-based simulations with explicit genetics (see the Appendix for simulation method), to investigate the robustness of some of our results to violations of the simplifying assumptions that were made above in order to get analytical results. Specifically, our analytical results neglected all sources of stochasticity other than the effect of the randomly changing environment, namely: (i) random genetic drift in the mean and variance of the trait (Bürger and Lande 1994), and (ii) demographic stochasticity coming from the randomness in survival and fecundity not attributable to environmental variation (Lande et al. 2003). Random

genetic drift of the mean phenotype, assuming a constant genetic variance, is straightforward to include here, simply by replacing formulas for the variance and autocorrelation of deviations from the optimum (eqs 9a,b) by their equivalent accounting for drift (see Table 1 in Chevin & Haller 2014). In contrast, there is no simple prediction for the variance and autocorrelation of the additive genetic variance G under genetic drift and stabilizing selection. This is important to investigate, as the variance in G causes stochasticity in responses to selection even in a constant environment, which should amplify the variance in fitness, and ultimately in population size, relative to our prediction in eq. (6b).

Figure 6A shows that the mean log-population size across replicate individual-based simulations of density-independent growth (far below the ceiling carrying capacity) is well predicted by our analytical predictions in eq. (6A), replacing the constant genetic variance by its expectation from the house-of-cards approximation, $G_{HC} = 0.5$. The autocorrelation in the optimum phenotype has highly non-linear effects on the expected log population size: curves for $\rho = 0.1$ and $\rho = 0.5$ are barely distinguishable, while they both differ from that for $\rho = 0.9$. Our analytical results also perform well for the variance in ln$N$, as shown by Fig 6B. This indicates that the variance caused by other sources of stochasticity (fluctuations in G, demographic stochasticity) does not strongly alter our predictions, in conditions where drift is not prevalent, and when the trait is determined by a large number of loci. Comparison of Figure 6B with Fig 6A further shows that autocorrelation in the optimum phenotype has a much stronger effect on the variance than it has on the expectation of ln$N$.

We also examined skewness of ln$N$ (Fig. 6C), and found that the quantitative agreement with predictions is not as good as for the mean and variance. This was somewhat anticipated, because (i) estimation of the third moment requires larger sample size, which were difficult to achieve with individual-based simulations; (ii) we did not start from a constant population size (as required for our predictions), but from a distribution skewed by the ceiling density dependence during the burn-in period; and (iii) the skewnesses from different processes (density-dependent burn-in versus density-independent simulation) are not additive, so the effect of initial conditions is not removed by rescaling by lnN_0 (contrary to the mean and variance). Nevertheless, the main features we describe analytically (based on the gamma approximation) were correctly found, with accuracy increasing in time past a few generations dominated by the influence of initial conditions. Specifically, the log-population sizes were skewed negatively,

with larger negative skew under higher autocorrelation in the optimum, and an absolute value that decreases with time (Fig. 6C).

Discussion

Summary of results

Skewed abundance distribution

We showed that when environmental stochasticity of population growth is caused by fluctuating selection in the form of a randomly changing optimum phenotype (as commonly modeled in evolutionary ecology), the distribution of population size on the log scale is well approximated by a reverse gamma distribution, with shape and scale that depend on the variance and autocorrelation of the optimum, and on genetic responses to selection. This distribution is skewed negatively, with an excess of low population sizes relative to a symmetric distribution with the same mean and variance. Phenomenological models of population dynamics often include environmental stochasticity by means of a normal distribution of Malthusian fitness (or correspondingly, a log-normal distribution of multiplicative fitness), which produces a normal distribution of the log population size (lognormal abundance distribution) in the contexts we investigated here (Lande et al. 2003). As shown in figure 1, the distribution of *lnN* conditional on initial size, describing multiple replicate populations starting from the same size (e.g. in laboratory experiments) or probabilistic projections for a single population with known size, can depart substantially from this normal prediction.

The excess of low population sizes is transient under density-independent population growth, but may still make a large difference for extinction risk, in contexts where transient dynamics matter. One such situation of particular interest is evolutionary rescue, where an abrupt environmental stress (beyond the random fluctuations) causes a population to decline, and face extinction unless it evolves rapidly enough (Bell and Gonzalez 2009; Gomulkiewicz and Holt 1995). Furthermore, we show analytically that a skewed stationary distribution is maintained asymptotically (in the long run) under Gompertz density dependence, while this form of density dependence would lead to a normal distribution of populations size under the phenomenological model of environmental stochasticity, and ignoring temporal autocorrelation (Lande et al. 2003). We also show that the skewness of the equilibrium distribution of population size increases with

increasing temporal autocorrelation in the optimum and strength of density dependence. The latter occurs because, under stronger density dependence, current population size is less influenced by the past history of maladaptation.

Dual role of environmental autocorrelation

Our analysis also highlights a dual role of temporal autocorrelation of the environment in driving the eco-evolutionary dynamics. On the one hand, when the optimum phenotype is more autocorrelated in time, it is tracked more closely by the evolutionary dynamics of the mean phenotype, thus reducing the expected lag load (Charlesworth 1993; Chevin 2013; Lande and Shannon 1996), and increasing the expected population size. But on the other hand, larger autocorrelation in the optimum causes higher stochastic variance in population dynamic paths (eq. 6b), which by itself can strongly increase extinction risk, because some populations may experience by chance a long series of bad years. The latter effect of autocorrelation of the optimum mirrors effects of autocorrelation of population growth rates previously described in phenomenological models of stochastic population dynamics (Johst and Wissel 1997; Laakso et al. 2003; Pike et al. 2004). However here, autocorrelation in fitness has a more complex dependence on environmental autocorrelation, since maladaptation also depends on evolutionary responses to selection.

Stochasticity in evolutionary rescue

Our results about evolutionary rescue (ER) following a major environmental shift show that environmental stochasticity can have a major detrimental impact on this process. First, random fluctuations in the optimum decrease the expected growth rate and population size (compare blue and black lines in figure 2B). And second, it causes stochastic variance in population size on the log scale, such that the population size can span several orders of magnitude (black quantile lines in figure 2B). Importantly, these effects act with equal strength in every generations (under stationary fluctuations), while the effect of the deterministic shift from the mean optimum decreases geometrically with time (figure 2A). As a consequence, when a deterministic shift in the optimum is combined with stochastic fluctuations, variance in the optimum strongly impacts extinction risk during ER, by increasing both the probability to reach a critically low population size, and the time spent near this low size (figure 3A). Autocorrelation in the optimum has a more moderate influence on ER as long as it remains at intermediate values, say, between 0.1

and 0.9 as in figure 3B, because this corresponds to moderate variation in the characteristic time of autocorrelation $T = -\ln(\rho)^{-1}$, which appears the evolutionary predictions in eqs. (9a,b). Overall, as randomness in the environment is probably ubiquitous in the wild (Vasseur and Yodzis 2004), and we show here that the stochastic component of fitness strongly impacts the outcome of ER (eq. 11, figures 3-5), any biological mechanism that may affect how environmental fluctuations translate into stochasticity in maladaptation and fitness, including phenotypic plasticity (Ashander et al. 2016 ; Michel et al. 2014; Reed et al. 2013) and/or bet hedging (Tufto 2015), is likely to have a strong impact on evolutionary rescue.

Robustness and generality

Alternative sources of skewness

Although the exact form of the distribution of population size we derive depends on the specific shape of the fitness function (Gaussian fitness peak), its most salient aspects are certainly robust to these assumptions. In particular, any fitness function with an optimum that changes with the environment is likely to lead to a distribution of population size that is bounded above by the cumulative growth rate of the optimum phenotype, and skewed negatively towards low population sizes. The same holds for tolerance curves representing fitness directly as a function of the environment (without measured traits under selection), which are typically concave, with an optimum environment where fitness is maximized. In fact, our results readily apply to such tolerance curves, as long as they can be approximated as Gaussian (or quadratic for Malthusian fitness) near the optimum environment (Chevin et al 2010 ; Lande 2014). It is important to note that density regulation can also cause skewness in the distribution of population size, especially in non-equilibrium situations where the population is expected to be well below carrying capacity, as occurs during evolutionary rescue (scenario underlying Figure 4). Density dependence also increases the skewness of the stationary distribution of population size around the carrying capacity under a fluctuating optimum (Figure 5). Investigating the relative contributions of density dependence versus a fluctuating optimum to skewness in the distribution of population size (say, across replicates of experimental evolution) thus requires controlling the strength of resource competition and other interactions contributing to density regulation. A skewed distribution of population size is more likely to be caused by fluctuations of an optimum

phenotype in populations that start at low size, where density-dependent competition can be neglected.

Changes in genetic variance and strength of selection

Our analytical predictions, despite assuming constant genetic variance, were matched reasonably well by individual-based simulations with explicit loci. Chevin & Haller (2014) similarly observed that the temporal distribution of selection gradients and deviations from the optimum in individual-based simulations are well captured by theory that assumes constant genetic variance. One of the reasons why the approximation performs well is because we modeled a rather large number of loci, and chose parameter values so as to yield realistic levels of heritability ($h^2 = 1/3$), mutational variance ($V_m = 10^{-3} V_e$), and per-gene mutation rates (10^{-4}). These parameter values jointly lead to a moderate coefficient of variation of G over time (Bürger and Lande 1994). Fewer loci, and/or lower genomic mutation rates, may lead to more stochasticity in genetic variance and the responses to selection, thus inflating the stochastic variance in population size relative to our predictions. However, this would also involve moving away from the context of a polygenic quantitative trait, such that other eco-evolutionary models (e.g. Martin et al. 2013) would be more appropriate anyway.

We also assumed weak stabilizing selection, consistent with the available data on measurements of selection (Chevin et al. 2015; Johnson and Barton 2005; Kingsolver et al. 2001). Stronger stabilizing selection would not substantially alter our predictions, provided that the combination of selection strength with mutation rate and effects is such that the system allows for substantial genetic variance to be maintained (Johnson and Barton 2005), thus remaining within the realm of quantitative genetic theory. The continuous-time approximation underlying eq. (9), which requires weak stabilizing selection, can easily be replaced by a more accurate discrete-time version under stronger selection.

Empirical relevance

The parameters that enter the model can all be measured empirically, although some of them require large datasets. For instance, Chevin et al. (2015) recently showed that the variance and autocorrelation of an optimum phenotype in the form that is modeled here can be estimated from data on fitness and traits over time, using quadratic (Poisson) regression with a random effect on the slope. Estimating the additive genetic variance of a continuous trait based on the resemblance

between relatives is the main goal of quantitative genetics, and has been performed an enormous number of times in the laboratory and in the wild (reviewed by Charmantier et al. 2014; Falconer and MacKay 1996; Kruuk 2004; Lynch and Walsh 1998). The intrinsic rate of increase can be estimated from the individual vital rates using the Euler-Lotka equation (Kot 2001; Roff 2002), or from times series of population size starting at low density (Kot 2001). Time series of population sizes can also be used to measure the strength and functional form of density dependence (Coulson et al. 2008; Lebreton and Gimenez 2013).

Even assuming that these parameters can be estimated accurately, confronting predictions based on these measurements to actual population dynamics in a stochastic environment requires a large number of replicate populations in controlled environments, making experimental evolution with short-lived organisms the ideal system. On the other hand, if most elements of the model have been measured with some confidence, they can still be used to make projections for the fate of a single population in the wild. The component of uncertainty in these predictions caused by the randomness in environmental fluctuations can be included explicitly using the stochastic variance of population size predicted by the model (eq. 6b).

Conclusions

We have derived a set of predictions for the stochastic population dynamics generated by a moving optimum phenotype, which is the most common way of modeling adaptation to a changing environment in evolutionary ecology. Our results can serve as a baseline for comparison to more phenomenological models, where variation in population growth is postulated *a priori* without an explicit underlying mechanism. Beyond finding results in contexts that parallel those from phenomenological models, we also extend them, notably by characterizing the stationary distribution under (Gompertz) density dependence with environmental autocorrelation. Our hope is that our predictions will stimulate new empirical work, notably experimental evolution in the laboratory, towards a better understanding of eco-evolutionary dynamics in stochastic environments.

Acknowledgements

We thank L. Fouqueau for useful discussions and feedback, and R. Lande, S. R. Proulx and two anonymous reviewers for comments on this manuscript. L.-M. C and O. C. are supported by the

European Research Council (grant FluctEvol ERC-2015-STG-678140), and J. A. by the NSF IGERT program (J.A., DGE-0801430 to P.I. Strauss) and the Center for Population Biology at UC Davis.

APPENDIX

Derivation of the moments of *n* under Gompertz regulation

Under Gompertz regulation eq. (2) becomes

$$n_{t+1} = (1-\varphi) n_t + r_m - L_v - \frac{S}{2} x_t^2 . \tag{A1}$$

The solution to this difference equation is (for $t \geq 1$)

$$n_t = (1-\varphi)^t n_0 + \sum_{k=1}^{t} (1-\varphi)^{t-k} (r_m - L_v - \frac{S}{2} x_{t-1}^2) , \tag{A2}$$

which after summing the first geometric series becomes

$$n_t = (1-\varphi)^t n_0 + (r_m - L_v) \frac{1-(1-\varphi)^t}{\varphi} - \frac{S}{2} \sum_{j=0}^{t-1} (1-\varphi)^{t-(j+1)} x_j^2 . \tag{A3}$$

Assuming $1 < \varphi < 0$, this leads asymptotically to

$$n = \frac{r_m - L_v}{\varphi} - \frac{S}{2} \lim_{t\to\infty} \left(\sum_{j=0}^{t-1} (1-\varphi)^{t-(j+1)} x_j^2 \right). \tag{A4}$$

From eq. (A4), the asymptotic mean log population size under Gompertz regulation and a fluctuating optimum causing a stationary distribution of maladaptation *x* is

$$\mathrm{E}(n) = \frac{r_m - L_v}{\varphi} - \frac{S\sigma_x^2}{2} \lim_{t\to\infty} \left(\sum_{j=0}^{t-1} (1-\varphi)^{t-(j+1)} \right). \tag{A5}$$

Summing the geometric series and taking the limit for large *t* leads to

$$\mathrm{E}(n) = \frac{r_m - L_v - S\sigma_x^2 / 2}{\varphi} , \tag{A6}$$

which leads to formula (12a) in the main text after replacing $\varphi = r_m / \ln K_m$. The stationary variance of log population size is

$$\mathrm{V}(n) = \frac{S^2}{4} \lim_{t\to\infty} \left(\sum_{j=0}^{t-1} (1-\varphi)^{2[t-(j+1)]} \mathrm{V}(x_k^2) + 2 \sum_{i=0}^{\infty} \sum_{j=i+1,}^{\infty} (1-\varphi)^{2t-(i+j+2)} \mathrm{Cov}(x_i^2, x_j^2) \right), \tag{A7}$$

which can also be written as

$$\mathrm{V}(n) = \frac{S^2\sigma_x^4}{2}\left[\frac{1}{\varphi(2-\varphi)} + 2\lim_{t\to\infty}\left(\sum_{i=0}^{t-1}\sum_{j=i+1,}^{t-1}(1-\varphi)^{2t-(i+j+2)}\,\mathrm{Corr}(x_i^2, x_j^2)\right)\right] \qquad \text{(A8)}$$

where Corr() denotes a correlation and we have used the fact that $\mathrm{V}(x^2) = 2\sigma_x^4$ because *x* is a centered normal variable. We also have $\mathrm{Corr}(x_i^2, x_j^2) = \mathrm{Corr}(x_i, x_j)^2 = Y_{ij}^2$, and using the approximation (9c) in the main text, the term in the sum in (A8) becomes $\left((1-\varphi)^{t-(\frac{i+j}{2}+1)}\,U^{|i-j|}\right)^2$.

Summing from 0 to $t-1$ and taking the limit for large *t* yields, after some algebra,

$$\sum_{i=0}^{t-1}\sum_{j=i+1,}^{t-1}(1-\varphi)^{2t-(i+j+2)}\,\mathrm{Corr}(x_i^2, x_j^2) \approx \frac{2U^2(\phi-1)}{[1+U^2(\phi-1)](\phi-2)\phi}. \qquad \text{(A9)}$$

Summing with the other term $1/[\varphi(2-\varphi)]$ produces the formula for the variance in the main text.

The form of the distribution can be found by noting that, from eq. (A5), the stationary distribution of log population size in the long run under Gompertz regulation is proportional to a weighted sum of squared deviations from optimum in past generations, which is again well approximated by a gamma distribution under a Gaussian process for the optimum. The shape and scale of this gamma are found by matching moments of the quadratic form, as done for eq. (7).

To find the autocorrelation of the stationary distribution, we start by writing, using eq. (A3),

$$\begin{aligned}\mathrm{Cov}(n_t, n_{t+\tau}) &= \frac{S^2}{4}\mathrm{Cov}\left(\sum_{i=0}^{t-1}(1-\varphi)^{t-(i+1)}\,x_i^2, \sum_{j=0}^{t+\tau-1}(1-\varphi)^{t+\tau-(j+1)}\,x_j^2\right)\\ &= \frac{S^2\sigma_x^4}{2}\sum_{i=0}^{t-1}\sum_{j=0}^{t+\tau-1}(1-\varphi)^{2t+\tau-(i+j)-2)}\,\mathrm{Corr}(x_i^2, x_j^2) \qquad \text{(A10)}\\ &\approx \frac{S^2\sigma_x^4}{2}\sum_{i=0}^{t-1}\sum_{j=0}^{t+\tau-1}(1-\varphi)^{2t+\tau-(i+j)-2)}\,U^{2|i-j|}\end{aligned}$$

where in the last line we have used the approximation (9c) for $\mathrm{Corr}(x_i^2 x_j^2)$. Because of the absolute value in (A10), computation of the sum above requires separation into three sums, *A*, *B*, and *C*, respectively for $i = j$, $i < j$ and $i > j$. Specifically, we have

$$A = \sum_{i=0}^{t-1}(1-\varphi)^{2t+\tau-2i-2)}$$

$$B = \sum_{i=0}^{t-1} \sum_{j=i+1}^{t+\tau-1} (1-\varphi)^{2t+\tau-(i+j)-2} U^{2(i-j)} \quad \text{(A11)}$$

$$C = \sum_{i=0}^{t-1} \sum_{j=0}^{i-1} (1-\varphi)^{2t+\tau-(i+j)-2} U^{2(j-i)}$$

Summing the geometric series, taking the limit for large *t*, and dividing by the variance yields, after some algebra, the formula in eq. (14) for the autocorrelation of log population size τ generations apart.

Simulation methods

Population-based simulations

Population-based simulations consisted of recursions of the eco-evolutionary equations, whereby phenotypic change followed the standard $\Delta\bar{z} = -GS(\bar{z} - \theta)$ assuming constant genetic variance, and population dynamics followed equation (1). We simulated a first-order autoregressive process (AR1) for the optimum phenotype with mean 0, variance σ_θ^2, and autocorrelation ρ, by (i) drawing the optimum in the first generation from a Gaussian with mean 0 and variance σ_θ^2, and (ii) drawing the optimum in each generation $t > 0$ as $\theta_t = \rho\theta_{t-1} + \sqrt{1-\rho^2}u_t$, where u_t is also drawn from a Gaussian with mean 0 and variance σ_θ^2. The initial mean phenotype was assumed to have reached a stationary response to the randomly changing optimum, such that the stochastic variance of the mean phenotype, and its covariance with the optimum, both correspond to analytical predictions from earlier theory (Chevin and Haller 2014; Lande and Shannon 1996). Specifically, the stochastic variance of the mean phenotype and its covariance with the optimum both equal $\sigma_\theta^2 SGT/(1+SGT)$, where $T = -1/\ln\rho$ (see also below), so the regression slope of $\bar{z}$ on θ is $r_{z,\theta} = SGT/(1+SGT)$. The initial mean phenotype was thus drawn as $\bar{z}_0 = r_{z,\theta}\theta_0 + \sqrt{1-r_{z,\theta}}\upsilon$, where υ was drawn from a normal distribution with mean 0 and variance $\sigma_\theta^2 SGT/(1+SGT)$.

Individual-based simulations

Individual-based simulations were performed with the program Nemo (Guillaume and Rougemont 2006). We considered a panmictic population of hermaphroditic individuals (mating system 6 in Nemo), with non-overlapping generations. We modeled a single quantitative trait under the control of $\ell = 50$ unlinked and additive diploid loci, such that the phenotype of an individual was given by the sum of allelic effects at each locus (genotypic value), plus a random environmental component drawn from a standard Gaussian distribution with variance $V_e = 1$. Mutations occurred at rate $u = 10^{-4}$ per haploid locus, and caused the allelic value to be incremented by an amount α drawn from a Gaussian distribution, with mean zero and variance $V_\alpha = 0.1$. These parameter values were chosen so as to yield realistic values (as reviewed by, e.g., Johnson and Barton 2005) for the mutational variance ($V_m = 2\ell u V_\alpha = 10^{-3} V_e$) and the heritability of the trait ($h^2 = G/V_e \approx 1/3$, see below).

Viability selection was implemented following equation (1) with $R_m = 1.25$, $\omega^2 = 25$, and density regulation of the ceiling form. Specifically, if the number of individuals in the new generation following reproduction exceeded the carrying capacity K, the population was culled to $N = K$ by removing randomly chosen individuals. We let the simulations run for 7999 generations with carrying capacity $K_0 = 3000$, to allow the genetic variance to reach an equilibrium between mutation, genetic drift, and stabilizing/fluctuating selection (burn-in period; we visually verified that this equilibrium had been achieved). Then at generation 8000, we increased the ceiling carrying capacity to $K = 10^5$ and followed the exponential growth of the population. We then computed moments of the distribution of the logarithm of population size across replicates at different times. These simulated moments were compared to the analytical predictions in eq. (6) below. For the analytical predictions, the additive genetic variance G we used was the theoretical prediction for the genetic variance under mutation and stabilizing selection in constant environment. Although a general formula exists that accounts for random genetic drift and interpolates between different approximations that function in different mutational regimes (stochastic house of Gauss, Hermisson and Wagner 2004), with our choice of parameters we could reliably use the simpler house-of-card approximation (Bürger and Lande 1994; Turelli 1984), $G_{HC} = 4\ell u V_\alpha / S \approx 0.5$. Because the initial population size was not constant in our simulation, but instead distributed below (and close to) the burn-in ceiling population size

(K_0 = 3000), the mean and variance were computed for the difference between final and initial log population size. Finally, in formulas that use $tr(\mathbf{Y}_t^2)$, we used the exact $\mathrm{E}(\lambda^2)$ rather than the approximation $1+\mathrm{V}_\lambda$ (below eq. 5a), because the latter performs less well in early generations, which were our focus in the simulations.

The codes for performing and analyzing the population- and individual-based simulations underlying our figures are deposited in the Dryad Digital Repository, doi:10.5061/dryad.101h0 (Chevin et al 2017).

Literature cited

Arnold, S. J., M. E. Pfrender, and A. G. Jones. 2001. The adaptive landscape as a conceptual bridge between micro- and macroevolution. Genetica 112:9-32.

Ashander, J., L. M. Chevin, and M. Baskett. 2016 Predicting rescue via evolving plasticity in stochastic environments. Proceedings of the Royal Society Series B-Biological Sciences.

Beissinger, S. R., and D. R. McCullough. 2002, Population viability analysis, University of Chicago Press.

Bell, G., and A. Gonzalez. 2009. Evolutionary rescue can prevent extinction following environmental change. Ecol Lett 12:942-948.

Boyce, M. S. 1992. Population viability analysis. Annual Review of Ecology and Systematics 23:481-506.

Bürger, R., and R. Lande. 1994. On the Distribution of the Mean and Variance of a Quantitative Trait under Mutation-Selection-Drift Balance. Genetics 138:901-912.

Bürger, R., and M. Lynch. 1995. Evolution and extinction in a changing environment - a quantitative-genetic analysis. Evolution 49:151-163.

Case, T. J., and M. L. Taper. 2000. Interspecific competition, environmental gradients, gene flow, and the coevolution of species' borders. American Naturalist 155:583-605.

Charlesworth, B. 1993. The evolution of sex and recombination in a varying environment. J Hered 84:345-350.

Charmantier, A., D. Garant, and L. E. Kruuk. 2014, Quantitative genetics in the wild, Oxford University Press.

Chevin, L. M. 2013. Genetic constraints on adaptation to a changing environment. Evolution 67:708-721.

Chevin, L.M., Cotto, O., J. Ashander. 2017. Data from: Stochastic evolutionary demography under a fluctuating optimum phenotype. American Naturalist, Dryad Digital Repository, DOI: doi:10.5061/dryad.101h0

Chevin, L. M., R. Gallet, R. Gomulkiewicz, R. D. Holt, and S. Fellous. 2013. Phenotypic plasticity in evolutionary rescue experiments. Philos Trans R Soc Lond B Biol Sci 368:20120089.

Chevin, L. M., and B. C. Haller. 2014. The temporal distribution of directional gradients under selection for an optimum. Evolution 68:3381-3394.

Chevin, L. M., and R. Lande. 2010. When do adaptive plasticity and genetic evolution prevent extinction of a density-regulated population? Evolution 64:1143-1150.
Chevin, L.-M., R. Lande, and G. M. Mace. 2010. Adaptation, plasticity, and extinction in a changing environment: towards a predictive theory. PLoS Biology 8:e1000357.
Chevin, L. M., M. E. Visser, and J. Tufto. 2015. Estimating the variation, autocorrelation, and environmental sensitivity of phenotypic selection. Evolution 69:2319-2332.
Coulson, T., T. Ezard, F. Pelletier, G. Tavecchia, N. Stenseth, D. Childs, J. G. Pilkington et al. 2008. Estimating the functional form for the density dependence from life history data. Ecology 89:1661-1674.
Coulson, T., and S. Tuljapurkar. 2008. The dynamics of a quantitative trait in an age-structured population living in a variable environment. Am Nat 172:599-612.
Ellner, S. P., M. A. Geber, and N. G. Hairston, Jr. 2011. Does rapid evolution matter? Measuring the rate of contemporary evolution and its impacts on ecological dynamics. Ecol Lett 14:603-614.
Engen, S., T. Kvalnes, and B. E. Sæther. 2014. ESTIMATING PHENOTYPIC SELECTION IN AGE-STRUCTURED POPULATIONS BY REMOVING TRANSIENT FLUCTUATIONS. Evolution 68:2509-2523.
Engen, S., R. Lande, and B.-E. Sæther. 2013. A quantitative genetic model of r-and K-selection in a fluctuating population. The American Naturalist 181:725-736.
Engen, S., R. Lande, and B. E. Saether. 2011. Evolution of a plastic quantitative trait in an age-structured population in a fluctuating environment. Evolution 65:2893-2906.
Engen, S., R. Lande, B. E. Sæther, and F. S. Dobson. 2009. Reproductive Value and the Stochastic Demography of Age-Structured Populations. The American Naturalist 174:795-804.
Engen, S., and B. E. Saether. 2014. Evolution in fluctuating environments: decomposing selection into additive components of the Robertson-Price equation. Evolution 68:854-865.
Estes, S., and S. J. Arnold. 2007. Resolving the paradox of stasis: models with stabilizing selection explain evolutionary divergence on all timescales. American Naturalist 169:227-244.
Falconer, D. S., and T. F. MacKay. 1996, Introduction to quantitative genetics. Harlow, UK, Longman Group.
Gilpin, M. E., and F. J. Ayala. 1973. Global models of growth and competition. Proceedings of the National Academy of Sciences 70:3590-3593.
Gomulkiewicz, R., and R. D. Holt. 1995. When Does Evolution by Natural Selection Prevent Extinction. Evolution 49:201-207.
Gomulkiewicz, R., R. D. Holt, M. Barfield, and S. L. Nuismer. 2010. Genetics, adaptation, and invasion in harsh environments. Evolutionary Applications 3:97-108.
Gomulkiewicz, R., and D. Houle. 2009. Demographic and genetic constraints on evolution. American Naturalist 174:E218-E229.
Guillaume, F., and J. Rougemont. 2006. Nemo: an evolutionary and population genetics programming framework. Bioinformatics 22:2556-2557.
Halley, J. M. 1996. Ecology, evolution and 1f-noise. Trends in Ecology & Evolution 11:33-37.
Hermisson, J., and G. P. Wagner. 2004. The population genetic theory of hidden variation and genetic robustness. Genetics 168:2271-2284.

Johnson, T., and N. H. Barton. 2005. Theoretical models of selection and mutation on quantitative traits. Philosophical Transactions of the Royal Society of London B: Biological Sciences 360:1411-1425.
Johst, K., and C. Wissel. 1997. Extinction risk in a temporally correlated fluctuating environment. Theoretical Population Biology 52:91-100.
Kingsolver, J. G., H. E. Hoekstra, J. M. Hoekstra, D. Berrigan, S. N. Vignieri, C. E. Hill, A. Hoang et al. 2001. The strength of phenotypic selection in natural populations. American Naturalist 157:245-261.
Kirkpatrick, M., and N. H. Barton. 1997. Evolution of a species' range. American Naturalist 150:1-23.
Kot, M. 2001, Elements of mathematical ecology, Cambridge Univ Pr.
Kruuk, L. E. B. 2004. Estimating genetic parameters in natural populations using the 'animal model'. Philosophical Transactions of the Royal Society of London Series B-Biological Sciences 359:873-890.
Laakso, J., K. Löytynoja, and V. Kaitala. 2003. Environmental noise and population dynamics of the ciliated protozoa Tetrahymena thermophila in aquatic microcosms. Oikos 102:663-671.
Lande, R. 1976. Natural selection and random genetic drift in phenotypic evolution. Evolution 30:314-334.
—. 1988. Genetics and demography in biological conservation. Science 241:1455-1460.
—. 1993. Risks of Population Extinction from Demographic and Environmental Stochasticity and Random Catastrophes. American Naturalist 142:911-927.
Lande, R., S. Engen, and B.-E. Sæther. 2009. An evolutionary maximum principle for density-dependent population dynamics in a fluctuating environment. Philosophical Transactions of the Royal Society B 364:1511-1518.
Lande, R., S. Engen, and B.-E. Saether. 2003, Stochastic population dynamics in ecology and conservation: an introduction. Oxford, UK, Oxford University Press.
Lande, R., and S. Shannon. 1996. The role of genetic variation in adaptation and population persistence in a changing environment. Evolution 50:434-437.
Lande, R. 2014. Evolution of phenotypic plasticity and environmental tolerance of a labile quantitative character in a fluctuating environment. Journal of Evolutionary Biology 27:866–875.
Lebreton, J. D., and O. Gimenez. 2013. Detecting and estimating density dependence in wildlife populations. The Journal of Wildlife Management 77:12-23.
Lynch, M., and R. Lande. 1993. Evolution and extinction in response to environmental change, Pages 234-250 *in* P. Kareiva, J. Kingsolver, and R. Huey, eds. Biotic Interactions and Global Change. Sunderland, Ma, Sinauer.
Lynch, M., and B. Walsh. 1998, Genetics and analysis of quantitative traits. Sunderland, MA, USA, Sinauer Associates. .
Martin, G., R. Aguilée, J. Ramsayer, O. Kaltz, and O. Ronce. 2013. The probability of evolutionary rescue: towards a quantitative comparison between theory and evolution experiments. Philosophical Transactions of the Royal Society B: Biological Sciences 368:20120088.
Martin, G., and T. Lenormand. 2006a. The fitness effect of mutations across environments: A survey in light of fitness landscape models. Evolution 60:2413-2427.

—. 2006b. A general multivariate extension of Fisher's geometrical model and the distribution of mutation fitness effects across species. Evolution 60:893-907.
Mathai, A. M., and S. B. Provost. 1992, Quadratic forms in random variables: theory and applications. New York, M. Dekker.
Michel, M. J., L. M. Chevin, and J. H. Knouft. 2014. Evolution of phenotype-environment associations by genetic responses to selection and phenotypic plasticity in a temporally autocorrelated environment. Evolution 68:1374-1384.
Orr, H. A., and R. L. Unckless. 2008. Population extinction and the genetics of adaptation. Am Nat 172:160-169.
Ozgul, A., D. Z. Childs, M. K. Oli, K. B. Armitage, D. T. Blumstein, L. E. Olson, S. Tuljapurkar et al. 2010. Coupled dynamics of body mass and population growth in response to environmental change. Nature 466:482-U485.
Ozgul, A., T. Coulson, A. Reynolds, T. C. Cameron, and T. G. Benton. 2012. Population Responses to Perturbations: The Importance of Trait-Based Analysis Illustrated through a Microcosm Experiment. The American Naturalist 179:582.
Pelletier, F., T. Clutton-Brock, J. Pemberton, S. Tuljapurkar, and T. Coulson. 2007. The evolutionary demography of ecological change: Linking trait variation and population growth. Science 315:1571-1574.
Pike, N., T. Tully, P. Haccou, and R. Ferrière. 2004. The effect of autocorrelation in environmental variability on the persistence of populations: an experimental test. Proceedings of the Royal Society of London B: Biological Sciences 271:2143-2148.
Ramsayer, J., O. Kaltz, and M. E. Hochberg. 2013. Evolutionary rescue in populations of Pseudomonas fluorescens across an antibiotic gradient. Evolutionary Applications 6:608-616.
Reed, T. E., V. Grotan, S. Jenouvrier, B. E. Saether, and M. E. Visser. 2013. Population growth in a wild bird is buffered against phenological mismatch. Science 340:488-491.
Ripa, J., and P. Lundberg. 1996. Noise colour and the risk of population extinctions. Proceedings: Biological Sciences:1751-1753.
Roff, D. A. 2002, Life history evolution. Sunderland, Massachusetts, Sinauer Associates
Ronce, O., and M. Kirkpatrick. 2001. When sources become sinks: Migrational meltdown in heterogeneous habitats. Evolution 55:1520-1531.
Ruokolainen, L., A. Linden, V. Kaitala, and M. S. Fowler. 2009. Ecological and evolutionary dynamics under coloured environmental variation. Trends in Ecology & Evolution 24:555-563.
Sæther, B.-E., T. Coulson, V. Grøtan, S. Engen, R. Altwegg, K. B. Armitage, C. Barbraud et al. 2013. How life history influences population dynamics in fluctuating environments. The American Naturalist 182:743-759.
Tufto, J. 2015. Genetic evolution, plasticity, and bet-hedging as adaptive responses to temporally autocorrelated fluctuating selection: A quantitative genetic model. Evolution 69:2034–2049.
Tuljapurkar, S. 1990, Population dynamics in variable environments. New York, Springer Verlag.
Turelli, M. 1984. Heritable genetic variation via mutation-selection balance: Lerch's zeta meets the abdominal bristle. Theoretical Population Biology 25:138-193.
Uecker, H., and J. Hermisson. 2016. The role of recombination in evolutionary rescue. Genetics 202:721-732.

Uyeda, J. C., T. F. Hansen, S. J. Arnold, and J. Pienaar. 2011. The million-year wait for macroevolutionary bursts. Proceedings of the National Academy of Sciences of the United States of America 108:15908-15913.
Vasseur, D. A., and P. Yodzis. 2004. The color of environmental noise. Ecology 85:1146-1152.
Wright, S. 1935. The analysis of variance and the correlations between relatives with respect to deviations from an optimum. Journal of Genetics 30:243-256.

Figure legends

Figure 1: distribution of log population size under density-independent growth. The distribution of population size n_t (conditional on initial population n_0) produced by stochastic fluctuations of an optimum phenotype with density-independent growth is shown for population-based recursions with constant genetic variance (5000 replicate populations, histogram), and the predicted gamma approximation (eq. 6-8, continuous line). The dashed line show a normal distribution with same mean and variance, as would be produced under the common assumption of a log-normally distributed multiplicative growth rates. The inset in the last panel shows a zoom on the smallest population sizes. Note that, because of the negative skew, the probability of low population sizes under a fluctuating optimum remains higher than under a Gaussian, even at relatively large times. Parameters are, height and width of the fitness function: $R_m = 1.1$ and $\omega = 5$; additive genetic and phenotypic variance: $G = 0.5$ and $P = 1$; variance and autocorrelation of the optimum: $\sigma_\theta^2 = 2$ and $\rho = 0.5$; and initial population size $N_0 = 1000$.

Figure 2. Evolutionary rescue in a stochastic environment. The eco-evolutionary dynamics following an abrupt environmental shift combined with stochastic environmental fluctuations of an optimum phenotype are shown, combining population-based simulations and analytical predictions. Panel A shows the optimum (gray lines) and the mean phenotype (black lines) for 5 representative simulation repeats, together with the analytical prediction (above eq. 10) for the expected mean phenotype over time (red line). Panel B shows the population dynamics. Individual paths of population size for each of the 500 simulation repeats are represented in gray, and the quantiles (0.01, 0.1, 0.25, 0.5, 0.75, 0.9, 0.99) of the distribution predicted by the

analysis (eqs. 6-8) are shown in black lines. The red line shows the expected trajectory with environmental stochasticity (from eq. 6a), while the blue line shows this same trajectory without any environmental stochasticity, as modeled by Gomulkiewicz & Holt (1995). The shaded zone represents a region of high extinction risk, below a critical population size of 100 (chosen arbitrarily). The optimum phenotype was shifted by $\delta = 4$ at generation 0, and also undergoes autoregressive fluctuations with variance $\sigma_\theta^2 = 1$ and autocorrelation over one generation $\rho = 0.7$. The maximum fitness is $R_m = 1.15$, the initial population size is $N_0 = 10000$, and all other parameters are as in Figure 1.

Figure 3. Extinction risk during evolutionary rescue in a stochastic environment. The probability P_{crit} that the population is below a critical size for extinction risk is represented over time for evolutionary rescue trajectories similar to those in Figure 2. Dots represent the proportion of simulated trajectories (out of 5000) where the population size is below N_c = 100. The continuous curves shows the prediction for this proportion P_{crit} (eq. 11). The variance of fluctuations in the optimum phenotype is varied in A: $\sigma_\theta^2 = 0.25$ (blue), 0.5 (cyan), 1 (green), 2 (orange), and 4 (red), with $\rho = 0.5$. The autocorrelation of fluctuations in the optimum phenotype is varied in B: $\rho = 0.1$ (blue), 0.5 (green), and 0.9 (red), with $\sigma_\theta^2 = 1$. The maximum multiplicative growth rate is $R_m = 1.2$, the shift in mean optimum is $\delta = 5$, and all other parameters are as in figure 2.

Figure 4. Density dependence and evolutionary rescue in a stochastic environment. The maximum probability P_{crit} that the population is below a critical size for extinction risk is

represented for population-based simulations of evolutionary rescue with varying forms of density dependence. The shape of the density dependence function was modified by changing the exponent Θ of a discrete-time version of Θ-logistic regulation (Θ = 1 is the Ricker model, a discrete-time analog of logistic regression). The rightmost point corresponds to ceiling regulation, where population growth is unlimited except at carrying capacity, and the dashed line shows the corresponding maximum P_{crit} under density-independent growth. The variance and autocorrelation of the optimum are $\sigma_\theta^2 = 1$ and $\rho = 0.5$, respectively, and all other parameters are as in figure 3.

Figure 5: Stationary distribution of population size with density dependence. The distribution of log-population size after 500 generations of eco-evolutionary dynamics under Gompertz density regulation is shown for 500 replicated population-based simulations (histograms), and compared to the predicted gamma distribution given by eqs (13a-b) (continuous black line). Insets show the autocorrelation of log-population size at different time intervals (in generations), for 10 replicate simulations (gray), together with the analytical prediction (eq. 14, continuous black line). The autocorrelation of log-population size was computed in a sliding window of 200 generations, over the last 9000 out of 10000 generations. The autocorrelation in the optimum phenotype was set to ρ = 0.1 (left) or ρ = 0.9 (right), and the strength of density dependence $\varphi = \ln R_m / \ln K_m$ is higher in the lower row. We have used $K_m = 10000$, and all other parameters are as in figure 4.

Figure 6. Individual-based simulations. The mean (A), variance (B), and skewness (C) of log-population size ln$N$ (scaled to the initial population size lnN_0) are shown for 475 replicate individual-based simulations of eco-evolutionary dynamics under a fluctuating optimum. The

trait is determined by 50 diploid loci, with mutation rate $\mu = 10^{-4}$ and variance of mutation effects $V_\alpha = 0.1$ per haploid locus, and the width of the fitness function is $\omega = 5$ (see Appendix 2 for more details). Results from simulations are shown as continuouss lines, while dashed lines show analytical predictions from eq. (6a), eq. (6b), and the gamma approximation $-\sqrt{8[1+\mathrm{V}_{\lambda,t-1}]/t}$ (below eq. 8b), respectively, replacing the constant genetic variance by the predicted additive genetic variance from the house-of-cards approximation, $G_{HC} = 0.5$ (Appendix 2). The initial population size is determined by the ceiling carrying capacity during the burn-in period, $K_0 = 3000$, which is well below the ceiling during the simulations, $K = 10^5$, such that population growth is essentially density independent after time 0. Gray levels correspond to different values of temporal autocorrelation in the optimum: $\rho = 0.1$ (light gray), 0.5 (dark gray) and 0.9 (black). Other parameters are $V_e = 1$ (residual phenotypic variance), $\sigma_\theta^2 = 4$ (variance of optimum), $R_m = 1.25$ (fecundity for optimum phenotype).

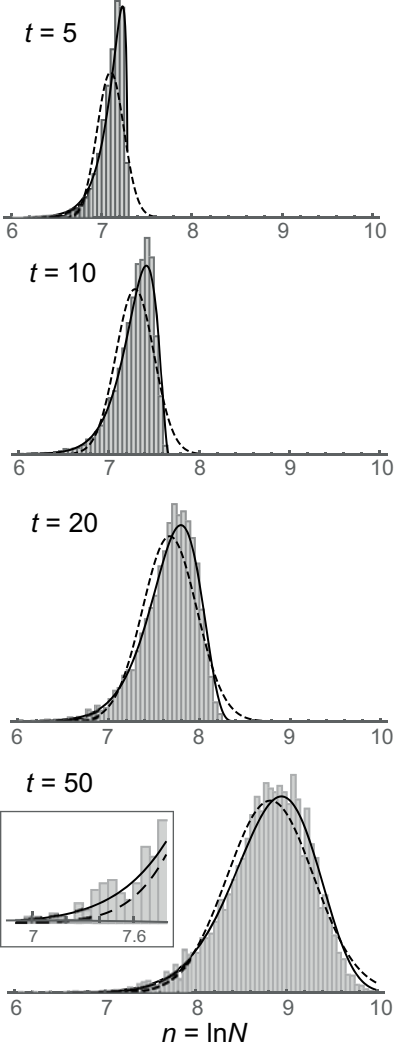
t = 5
6
7
8
9
10
t = 10
6
7
8
9
10
t = 20
6
7
8
9
10
t = 50
7
7.6
6
7
8
9
10
n = lnN

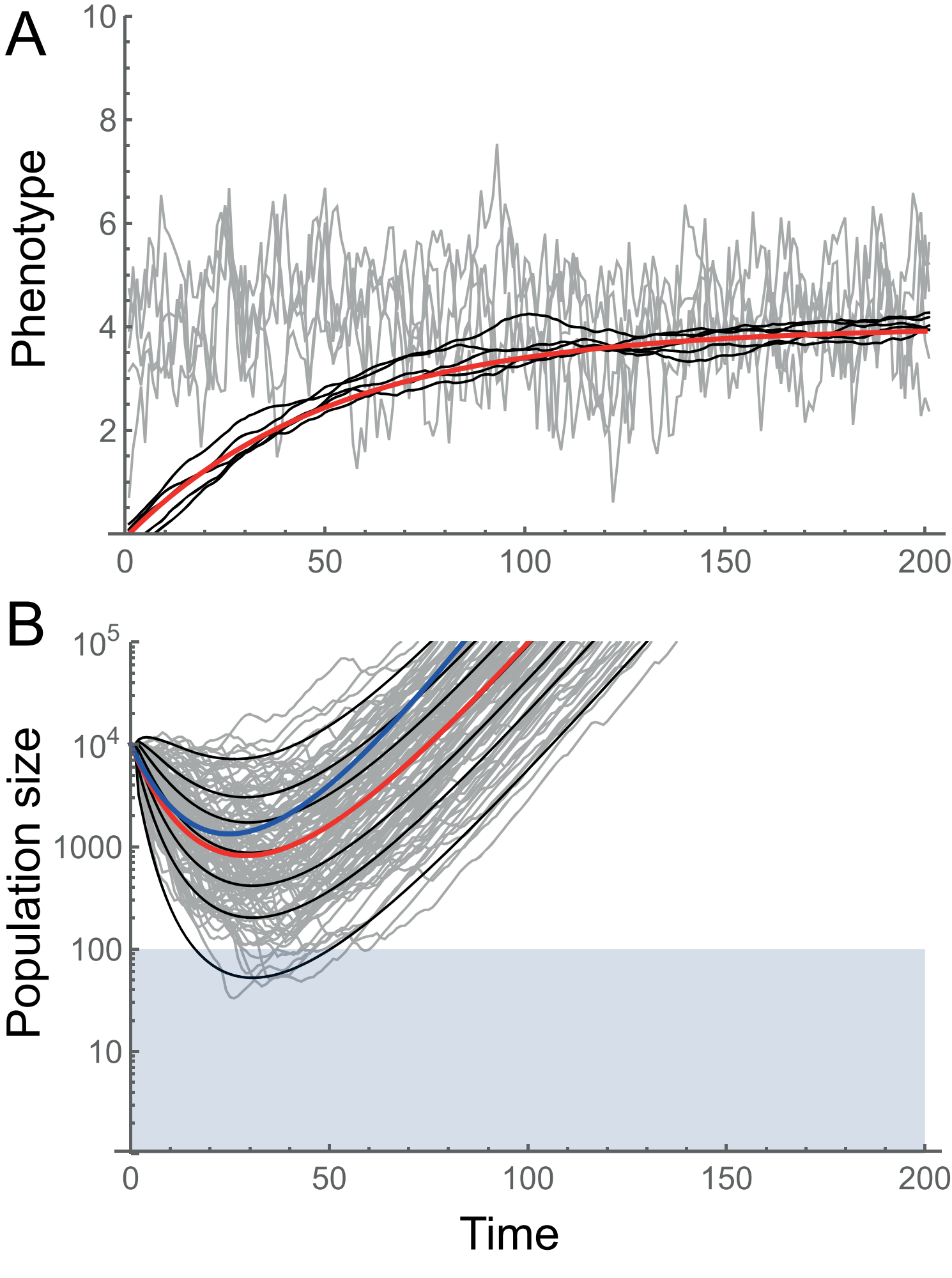
A
Phenotype
10
8
6
4
2
0
50
100
150
200
B
Population size
10^5
10^4
1000
100
10
0
50
100
150
200
Time

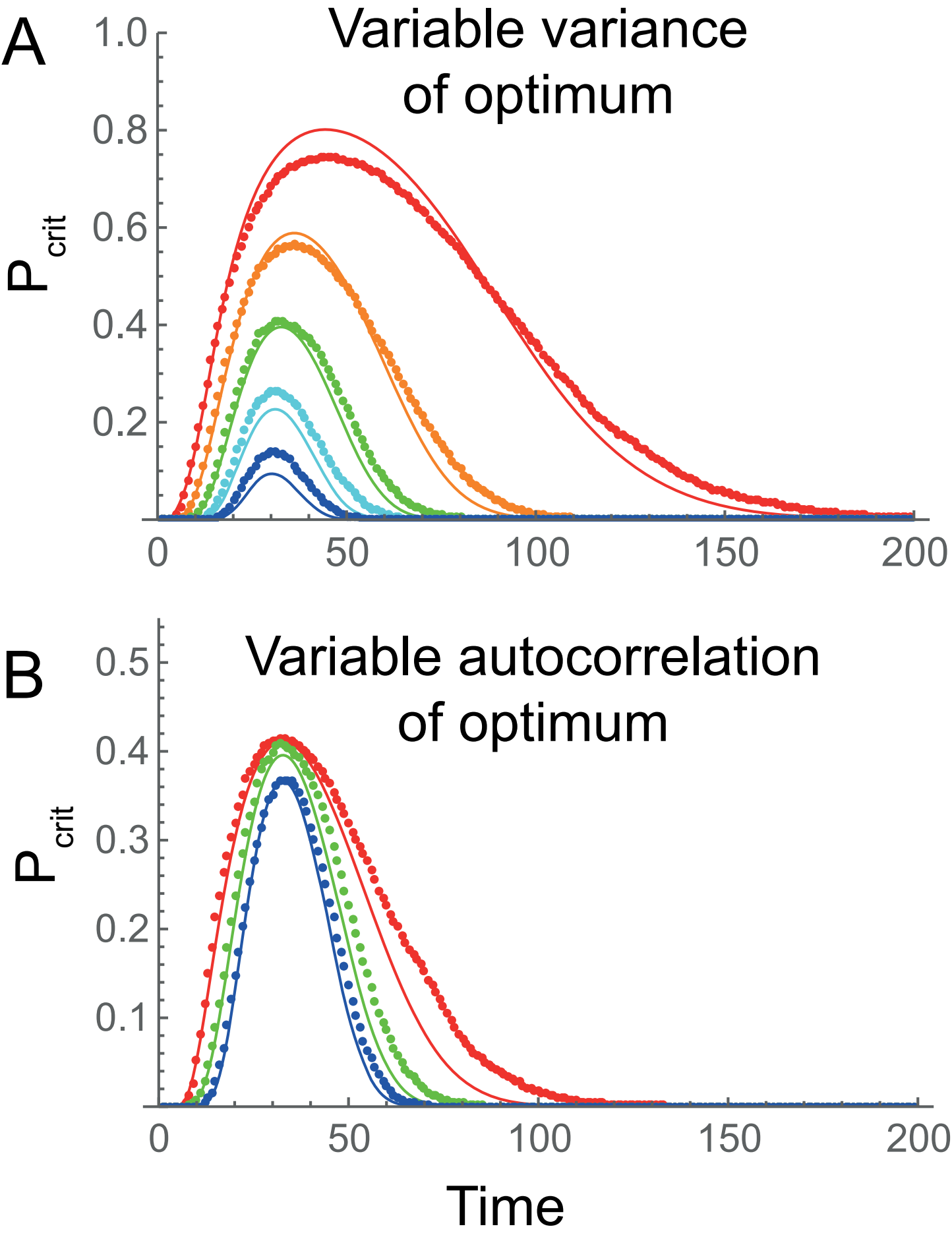
A
Variable variance of optimum
P_{crit}
1.0
0.8
0.6
0.4
0.2
0
50
100
150
200
B
Variable autocorrelation of optimum
P_{crit}
0.5
0.4
0.3
0.2
0.1
0
50
100
150
200
Time

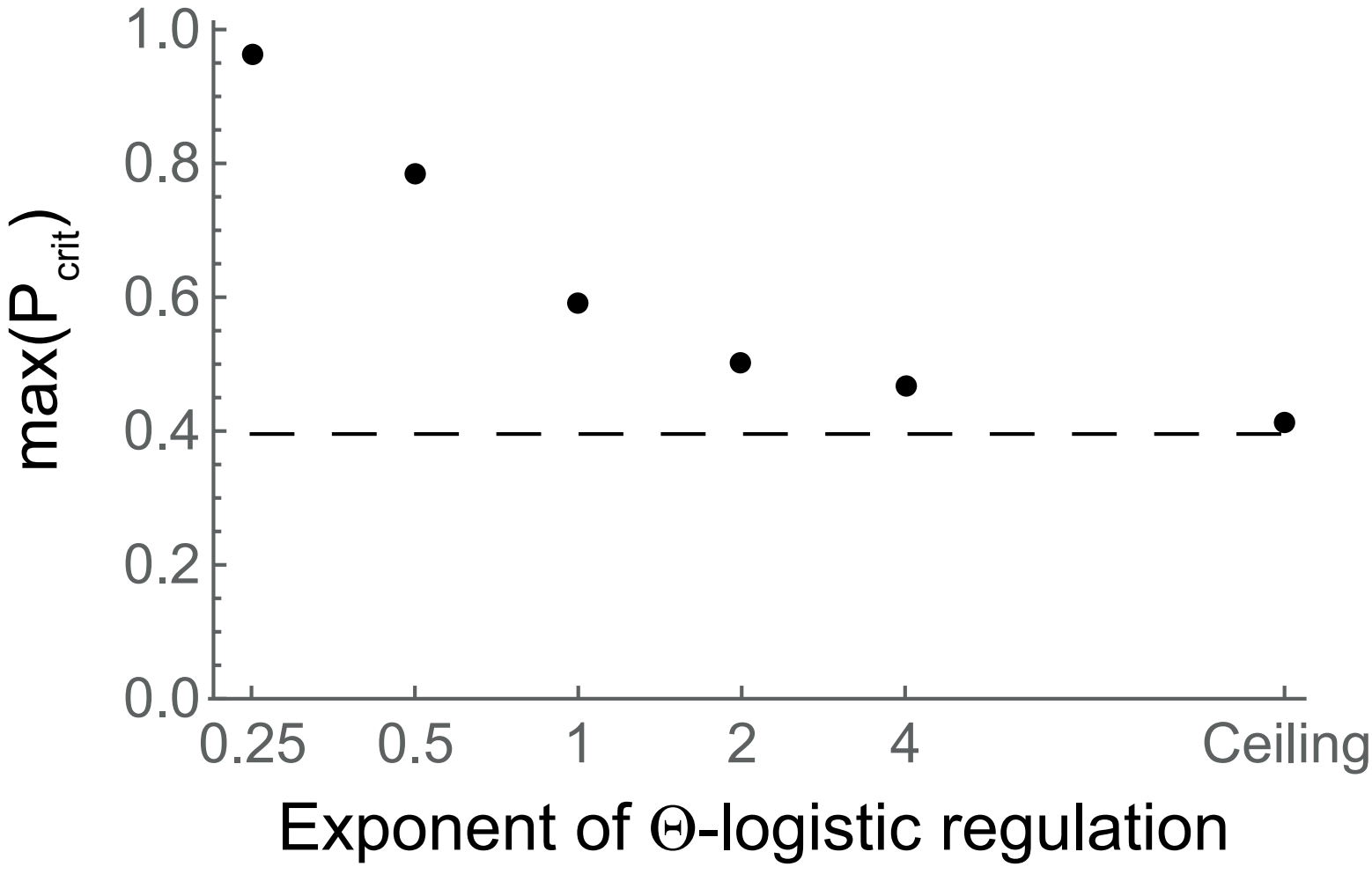
1.0
0.8
0.6
0.4
0.2
0.0
max(P_crit)
0.25
0.5
1
2
4
Ceiling
Exponent of Θ-logistic regulation

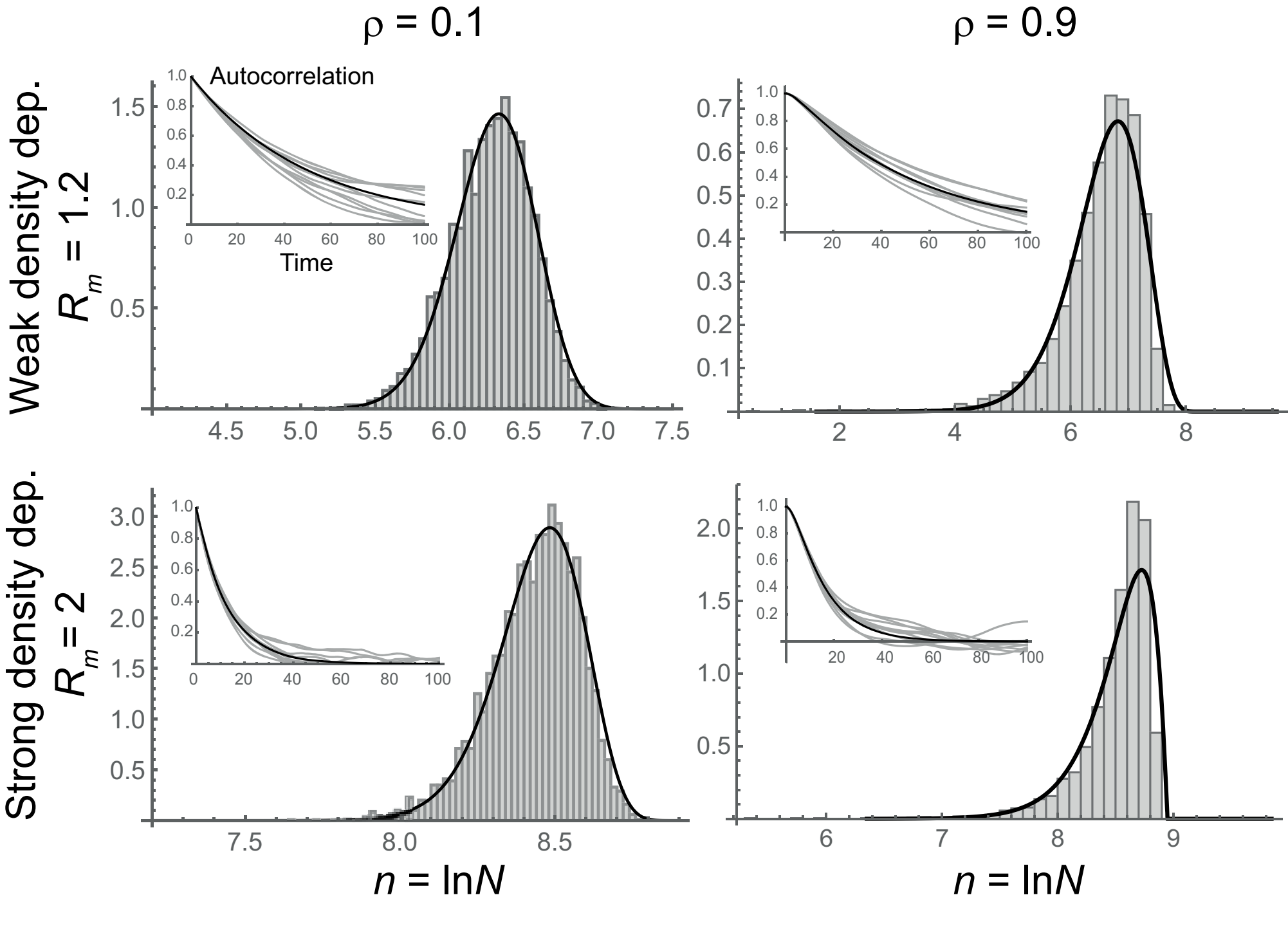
ρ = 0.1
ρ = 0.9
Weak density dep.
R_m = 1.2
Strong density dep.
R_m = 2
Autocorrelation
Time
n = ln$N$
n = ln$N$

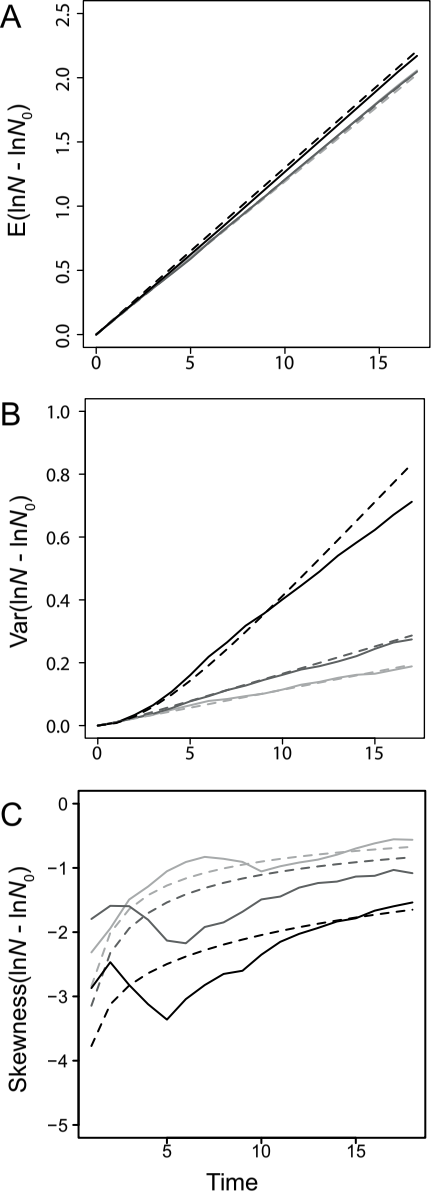
A
E(lnN - lnN0)
0.0
0.5
1.0
1.5
2.0
2.5
0
5
10
15
B
Var(lnN - lnN0)
0.0
0.2
0.4
0.6
0.8
1.0
0
5
10
15
C
Skewness(lnN - lnN0)
0
−1
−2
−3
−4
−5
5
10
15
Time